SHA
State Highway
Administration
Maryland Department of Transportation

Martin O'Malley, *Governor*
Anthony G. Brown, *Lt. Governor*

John D. Porcari, *Secretary*
Neil J. Pedersen, *Administrator*

STATE HIGHWAY ADMINISTRATION

RESEARCH REPORT

Estimation of Traffic Recovery Time for Different Flow Regimes on Freeways

Anthony A. Saka, PhD, PE, PTOE, PTP
Principal Investigator

Mansoureh Jeihani, PhD
Co-Principal Investigator

Petronella A. James
Doctoral Student, Lead Graduate Research Assistant

Department of Transportation and Urban Infrastructure Studies
School of Engineering
Morgan State University
Baltimore, MD 21251

SP708B4L
FINAL REPORT
July 2008

Technical Report Documentation Page

Report No. **MD-09-SP708B4L**	2. Government Accession No.	3. Recipient's Catalog No.
4. Title and Subtitle **Estimation of Traffic Recovery Time for Different Flow Regimes on Freeways**		5. Report Date **July 2008**
		6. Performing Organization Code
7. Author/s **Anthony A. Saka, Mansoureh Jeihani, and Petronella James**		8. Performing Organization Report No.
9. Performing Organization Name and Address **Department of Transportation and Urban Infrastructure Studies School of Engineering Morgan State University Baltimore MD 21251**		10. Work Unit No. (TRAIS)
		11. Contract or Grant No. **SP708B4L**
12. Sponsoring Organization Name and Address Maryland State Highway Administration, Office of Policy & Research 707 North Calvert Street , Baltimore MD 21202 National Transportation Center, Morgan State University 1700 East Cold Spring Lane, Baltimore, MD 21251		13. Type of Report and Period Covered **Final Report**
		14. Sponsoring Agency Code
15. Supplementary Notes		

16. **Abstract**

   This study attempts to estimate post-incident traffic recovery time along a freeway using Monte Carlo simulation techniques. It has been found that there is a linear relationship between post-incident traffic recovery time, and incident time and traffic intensity. For purposes of this paper, the post-incident recovery time is defined as that time beyond the clearing of an incident when pre-incident traffic conditions are achieved and traffic has returned to normalcy or steady state. The research supports Objective 2.1 of the SHA Business Plan, which seeks to develop measures to enhance the Maryland State Highway Administration's (SHA) ability to quantify the impact of congestion and delay on the highway network. In addition, the SHA understands that the capability to reasonably estimate the traffic recovery time for a given duration of incident is crucial in qualifying the cost-effectiveness of current/future traffic management programs involving detection and clearance of incident on freeways. A total of 121 traffic scenarios of traffic intensity (Rho), incident duration, and proportion of lane blockage were simulated resulting in a total of 726 experiments. The VISSIM simulation platform was used to derive values for output flow, density, and speed to determine the post-incident traffic recovery times. The analysis of simulated data showed that for a given incident duration and lane blockage scenario, the recovery time of the traffic increases non-linearly with traffic intensity. The traffic recovery time becomes uniform (stable) for low and moderate traffic intensity values. A set of linear regression models were developed to reasonably estimate the post-incident traffic recovery time using traffic intensity, incident duration, and proportion of lane blockage as exogenous variables.

17. Key Words: Simulation, congestion, incident time, traffic recovery time, traffic intensity, lane closure, non-recurring incidents	18. Distribution Statement: No restrictions **This document is available from the Research Division upon request**.		
19. Security Classification (of this report) **None**	20. Security Classification (of this page) **None**	21. No. Of Pages **67**	22. Price
Form DOT F 1700.7 (8-72) Reproduction of form and completed page is authorized.			

TABLE OF CONTENTS

LIST OF TABLES

LIST OF FIGURES

LIST OF APPENDICES

LIST OF EQUATIONS

ACKNOWLEDGEMENT

EXECUTIVE SUMMARY

This study attempts to estimate post-incident traffic recovery time along a freeway using Monte Carlo simulation techniques. It has been determined that a nonlinear relationship exists between post-incident traffic recovery time and incident time and traffic intensity (*v/c* ratio). In this study the post-incident recovery time is defined as that time beyond the clearing of an incident when pre-incident traffic conditions are achieved and traffic has returned to normalcy or steady state.

The research supports Objective 2.1 of the State Highway Administration's (SHA) Business Plan (2008-2011), which seeks to enhance the SHA's ability to quantify the impact of congestion and delay on the highway network. In addition, SHA understands that the ability to reasonably estimate the traffic recovery time for a given duration of incident is crucial in qualifying the cost-effectiveness of current and future traffic management programs involving detection and clearance of incidents on freeways.

This research is expected to benefit: (i) motorists who need to know how much delay to expect after an incident occurs and the time adjustments required to complete their journeys; (ii) transportation engineers and managers who need to be able to predict total incident in order to improve incident response and management; and (iii) intelligent transportation system (ITS) technologies, which are used to predict travel conditions.

In order to determine post-incident traffic recovery times, the VISSIM simulation model was used to derive values for output flow, density, and speed. Analysis of the simulated data showed that for a given incident duration and lane blockage scenario, the recovery time of the traffic increased nonlinearly with the traffic intensity. Additionally, the traffic recovery time approaches uniformity for low traffic intensity values.

In a total of 726 experiments, 121 traffic scenarios of traffic intensity (Rho-v/c ratio), incident duration, and proportion of lane blockage were simulated. Simulations were generated for three lane-blockage scenarios: three lanes blocked, two lanes blocked, and one lane blocked. The freeway segment used in the simulation was a 10-mile, three-lane, unidirectional straight section with no off-ramps, on-ramps, or bottlenecks such as lane drops and grades. Simulated capacity of the freeway was determined to be 2400 vehicles per hour per lane (vphpl). Vehicular traffic at near capacity (0.8<*Rho*<1.0), moderate (0.5<*Rho*≤ 0.80) and light (0.25≤*Rho*≤0.5) was allowed to enter the freeway on all lanes for 30 minutes prior to the incident in order to create a build-up of pre-incident steady stream traffic. On each lane, an incident was simulated by using a two-signal (red-green) traffic light, located at approximately mile seven on the 10-mile freeway. Incident duration ranged from 5 minutes to 60 minutes with 5-minute intervals for each level of traffic intensity.

Analysis of the simulated data for post-incident traffic recovery time showed a direct relationship between traffic intensity, incident duration, and recovery time. The results indicate that at each increase in traffic intensity level — with a corresponding increase in incident time — a higher post-incident recovery time is required for traffic to attain pre-incident travel conditions. In addition, within the same incident duration, recovery time increases proportionally as traffic intensity builds. However, recovery time

becomes indefinite as traffic intensity closely approaches the capacity threshold (Rho [ρ^0] = 1). Regression analysis confirms a nonlinear relationship between the three variables of traffic intensity, incident duration, and traffic recovery time. An adjusted R^2 of 0.851 supports the strength of the relationship between the variables for the aggregated data. Further analysis of the simulated traffic conditions suggests that the level of traffic intensity (*v/c*) is strongly and positively correlated with traffic recovery time for an adjusted R^2 of 0.926.

The ratio of traffic recovery time to incident duration increases nonlinearly for higher levels of traffic intensity and lane closure. For example, at *Rho* of 0.9 the recovery time was observed to be as high as approximately nine times the incident duration for 100 percent lane closure; six times incident duration for 67 percent lane closure; and three times incident duration for lane closure of 33 percent. In other words, depending on the proportion of lane closure, a five-minute incident at traffic intensity of 0.9 will likely result in delays ranging from 15-45 minutes. For *Rho* of 0.95, a recovery time as high as 15 times the incident duration was observed for 100 percent lane closure. This underscores the need to swiftly detect and clear incidents particularly during periods of high traffic intensity.

INTRODUCTION

Traffic managers are very familiar with the high financial, environmental, and social costs associated with delay engendered by nonrecurring incidents that impede the flow of traffic (i.e., lane blockage from construction activities, accidents, disabled vehicles, or natural phenomena). Many have postulated that the post-incident traffic recovery time exceeds the actual duration of an incident by a factor of four. While the above idea is clearly refutable because the recovery time is a function of the prevailing traffic intensity, it does have some element of truth regarding the relatively longer time period associated with traffic recovery in comparison to the actual duration of the incident. The probabilistic nature of most nonrecurring incidents makes it difficult to collect accurate empirical data that can be used in establishing a mathematical relationship between incident duration and traffic recovery time for different flow regimes or traffic intensity values. The duration of most nonrecurring incidents is usually unknown because of one's inability to determine the exact time of occurrence. Also, while accurate data can be collected on the actual duration of non-probabilistic incidents such as construction-related activities, multiple flow regimes are usually associated with these types of incidents because of their relatively long duration. Freeway incidents may include crashes, spilled loads, disabled or abandoned vehicles, vehicle fires, weather events, and temporary maintenance and construction activities. "Most of these incidents which can be described as random and unpredictable, significantly reduce freeway capacity and result in congestion" (Sung-Wai, Long and Der-Horng, 2004).

Freeway congestion is a major and costly problem in many U.S. cities and urban areas (Smith & Smith 2001). Congestion of any type results in costs to both users and system managers, such as longer travel times and lost productivity; air pollution and noise; reduced freeway capacity; and less efficient freeway operations (Smith & Smith 2001). The type of congestion most often encountered on freeways involves recurring congestion, which results from normal peak hour travel. However, nonrecurring congestion due to unpredictable incidents and events is equally, if not more, problematic than the familiar congested events. These nonrecurring incidents can cause large delays that contribute significantly to the total congestion experienced by travelers (Smith & Smith 2001).

It is not analytically plausible to develop a relationship between incident duration and traffic recovery time involving multiple flow regimes. The use of microscopic simulation provides the opportunity to generate pseudo-incidents for a variety of traffic-flow scenarios to facilitate a controlled study on the ramification of delay in responding to incidents on the highway network.

According to Smith and Smith (2001), the duration of an incident is composed of four important and distinct components: detection, response, clearance, and recovery (Figure 1). The recovery phase is defined as the period of time after the clearance of an incident for the traffic flow to return to a pre-incident steady state. The four phases together represent the total duration of the incident, or the period of time from the occurrence of an incident to the return of normal (steady state) traffic flow conditions.

Figure 1: The Four Phases of a Freeway Incident over Time (Smith & Smith 2001)
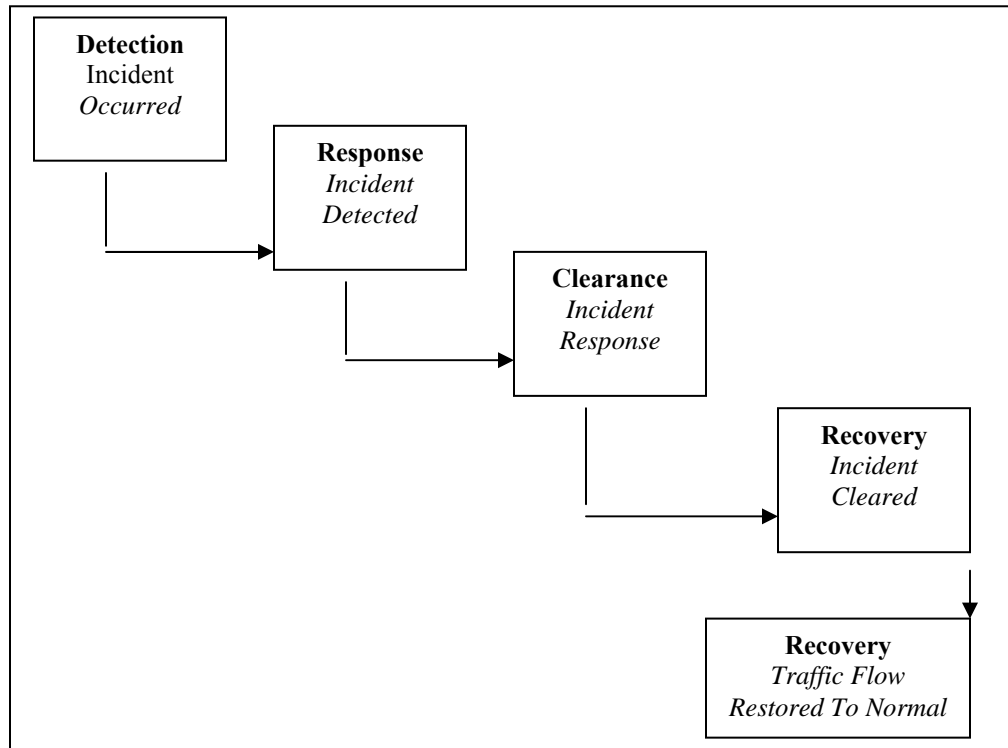
Objectives

The objectives of the project are:

- to develop, calibrate and validate a microscopic simulation model capable of reasonably depicting the prevailing traffic-flow conditions on selected segments of freeways with known design and operational parameters;

- to develop incident scenarios involving different durations and traffic intensities, and capture the resulting traffic recovery times; and

- to develop and document mathematical and/or graphical relationships between incident duration and traffic recovery time for different values of traffic intensity (i.e., volume-capacity ratio).

The research supports Objective 2.1 of the SHA Business Plan, which seeks to develop measures to enhance the SHA's ability to quantify the impact of congestion and delay on the highway network. In addition, the SHA understands that the capability of reasonably estimating the traffic recovery time for a given duration of an incident is crucial in qualifying the cost-effectiveness of current and future traffic management programs involving the detection and clearance of incidents on freeways. This research is expected to benefit: (i) motorists who need to know how much delay to expect after an incident occurs in order to adjust their journeys accordingly; (ii) transportation engineers and managers who must be able to predict total incident time (including traffic recovery to pre-incident steady state conditions) in order to improve incident response and management; and (iii) intelligent transportation systems (ITS) technologies that are used to reduce incident delay and predict travel conditions.

Scope

This study uses the VISSIM simulation platform to find a relationship between post-incident recovery time, incident time and traffic intensity on a freeway. The freeway segment used in the simulation is 10 miles in length, without off-ramps, on-ramps, or any other bottlenecks such as lane drops and grades. During the simulation no consideration was given to incident-induced rubbernecking activities. This was done to reduce the complexity of the analysis, and to create a simple model to serve as the reference base data. The assumed traffic stream in the simulation consisted of approximately 98 percent passenger cars, and 2 percent heavy-duty trucks, with one isolated incident per time and space. In other words, the impact of multiple incidents on congestion and recovery time was not included.

LITERATURE REVIEW

In order to provide an overall perspective on past research related to post-incident traffic recovery time (TRT) for different flow regimes on freeways, an extensive literature search was conducted. The literature search covered the operation and evaluation of freeway-incident management programs, different algorithms, and system tools, including simulation models developed for detecting and responding to freeway incidents. The main objectives of this review were to establish the originality of the study and obtain pertinent background information.

Operation and Evaluation of Incident Management Program

This aspect of the literature review focused on published efforts that are directed to the detection and clearing of incidents, and restoration of traffic flow.

The Coordinated Highway Action Response Team (CHART), a division of the Maryland State Highway Administration, published a report concluding that most incidents on the major commuting freeways in Maryland do not block traffic for more than one hour. The report focused on the state of Maryland's capability to timely detect and manage incidents on major freeways and highways. According to the CHART report, the three vital features associated with the efficiency of an incident management program are detection, response, and traffic recovery. Unfortunately, data needed for the execution of detection and response time analysis are not yet available under the CHART incident detection and response data [Chang and Point-du-Jour (2006)].

Bertini et al. (2005) documented how, archived ITS data in Portland, Ore., was used to evaluate the effectiveness of a freeway incident response program. The data showed various ways to present transportation information to indicate the effectiveness of an incident response program.

NCHRP Synthesis 318 (2003) profiled laws, policies, and procedures for facilitating safe and quick clearance of traffic incidents. These traffic incidents primarily included those initially blocking travel lanes on highways in urban and rural areas and attended to by the vehicle operator. The study also reported on national specific-site traffic incident clearance and investigation activities employed to quickly mitigate incidents of varying severity, from vehicle disablement to major or minor incidents.

Nee and Hallenbeck (2001) examined the similarities and differences among different service delivery modes including the intensity of deployment, equipment choices, service delivery and costs. They evaluated the impact of freeway service-patrol operation on traffic conditions (e.g., reductions in delay) and the level of motorist satisfaction.

Skabardonis et al. (1996) performed a study to evaluate the effectiveness of freeway service patrols on a section of Interstate 10 (Beat 8) in Los Angeles. An evaluation methodology was developed and used to estimate incident delays based on field data from loop detectors and probe vehicles to derive estimates of savings in performance measures.

Roper (1990) provided information on the procedures and processes that highway agencies use in responding to traffic congestion caused by incidents on freeways.

Algorithms and System Tools for Incident Management

Bertini and Myton (2005) described the evolution of traffic conditions over one morning peak period from freely flowing to congested conditions. This study confirmed the ability to identify freeway bottleneck activation without the pre-specification of incident on freeways. However, due to limitations in detector locations, it was difficult to draw major conclusions on bottleneck capacity.

Quiroga et al. (2005) developed a geographic information system based approach for the determination of patterns in the spatial and temporal distribution of incidents along freeway corridors.

Bertini et al. (2001) performed a statistical analysis of archived incident data for estimation of reductions in fuel consumption and delay, calculation of program costs, and development of a decision-making tool for design/expansion of corridors. Olmstead (2001) evaluated safety impacts of freeway management system using negative binomial regression.

Al-Deek (1999) tested the McMaster algorithm, an online state-of-the-art incident detection algorithm. Several factors were considered to determine their effects on the performance of the algorithm. These factors included the direction of travel and period of travel (peak vs. off-peak, sub-categorized by morning and evening).

Carvell et al. (1997) organized a freeway management handbook in modular fashion with each module addressing a particular aspect of technology or freeway management task. The modules were stand-alone treatments of particular areas of freeway management but were cross-referenced to reflect their interdependence.

Hall et al. (1993) sought to expand the understanding of freeway operations under congested conditions, with special emphasis on the flow-occupancy curve and the speed-flow curve. They suggested that modeling efforts encompass the aggregate traffic behavior under all operational conditions in order to provide better understanding of freeway operations under both free-flow and congested conditions.

Chang and Huang (1993) developed a knowledge-based expert system for microcomputers to assist in urban freeway incident management. They outlined the expert system, which included a graphics user interface, decision-making rules, and a knowledge inference mechanism to automate freeway- incident management applications. Chen et al. (2001) developed Performance Measurement System (PeMS) that extracts information from real-time and historical data. This system helped to obtain a uniform and comprehensive assessment of the performance of freeways.

Giuliano (1989) analyzed incident data and showed alternative approaches to reducing the congestion impacts of incidents on a Los Angeles freeway. The study described incident patterns and analyzed incident duration as a function of incident characteristics. Results from the analysis indicated that accidents make up a very small proportion of all incidents, but account for a relatively greater share of all incident duration.

Simulation Models in Incident Management

Ahmed and Cook (1980) formulated time-series analysis techniques for automatic detection of freeway capacity-reducing incidents. A series of papers — Nathanail and Zografos (1994, 1995), Zografos et al. (1993) and Zografos and Nathanail (1991) — have evaluated various aspects of the incident response and clearance process through analytical models that showed where to locate response units, which units to dispatch, and how to manage the process during clearance. From a more analytical perspective, Madanat (1996) modeled and simulated the incident response process to evaluate the effects of decisions made during different stages of the incident.

Various authors have developed expert systems to assist transportation management personnel in incident management, including the work of Gupta et al. (1992); Zhang and Ritchie (1992); Suttayamully et al (1995); and Hobeika (1996). Nathanail and Zografos (1995) proposed a framework to facilitate application of modeling and simulation to incident management. The framework addressed incident management on three axes – incident, domain, and lifecycle phase – and modeled and simulated across the incident management lifecycle.

In general, the vast majority of the articles, documents, and journals support the notion that effective incident management requires the three Cs: cooperation, coordination, and communication. From the available literature, there was no documentation on models for estimating post-incident traffic recovery time, which is valuable in determining the cost-effectiveness of operating freeway-incident management programs. Specifically, it is desirable for freeway-incident managers to associate economic and environmental cost with each minute of freeway incident. This rationalizes the need for programs that facilitate early detection, response, and clearance. Indeed, the delay from traffic back-ups associated with major traffic incidents is one of the most common concerns in freeway-traffic incident management because of the large number of people affected.

METHODOLOGY

Data Collection

As presented in Figure 2, the selected corridor is Interstate 83 between Exit 6 and Exit 1. Also known as the Jones Falls Expressway or JFX, I-83 serves as the major artery that connects the north Baltimore region to downtown Baltimore and primarily carries suburban commuter traffic to and from downtown Baltimore. Consequently, the peak direction of traffic on the JFX is southbound during the morning peak period and northbound during the evening peak period. The data collection included directional turning movements that were collected in 15-minute intervals for morning and evening peak hour periods; travel time data on the JFX; roadway geometric data; posted speed limits; and operating speeds. The peak-hour turning movements are in Appendix 1: *Summary of Morning Peak Hour Volumes on the JFX Corridor.* The morning and evening peak-hourly flow rates and associated peak hour factors (PHF) obtained from analyzing the raw data served as a guide in calibrating the simulation models.

Figure 2: JFX (I-83) Corridor (Exits 1 - 6) – in Baltimore, MD
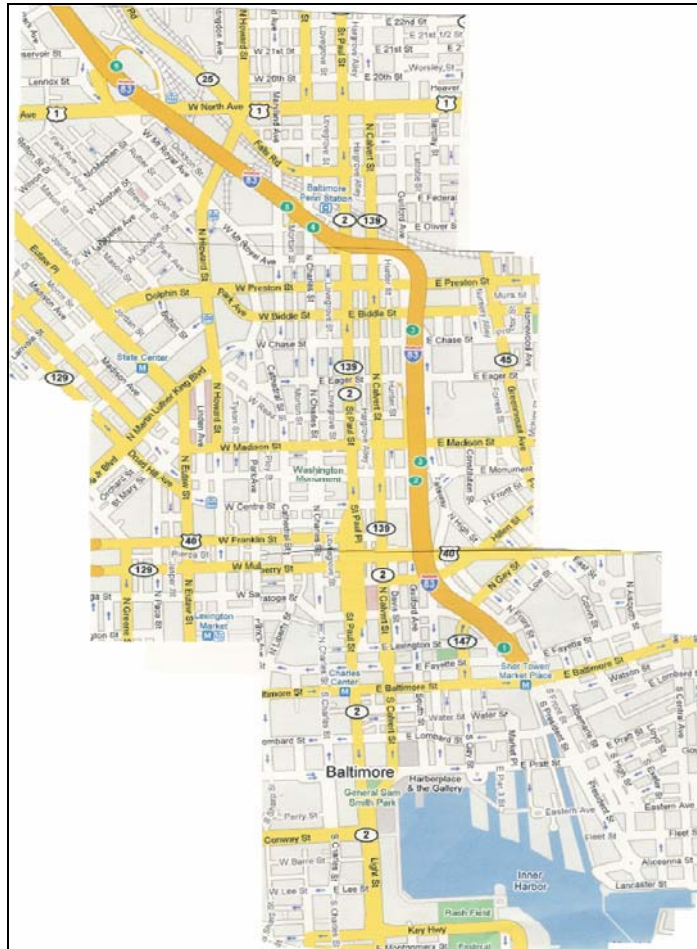
Development and Validation of Simulation Model

The simulation model used the VISSIM platform, a commonly utilized traffic simulation tool. The model utilizes network data (roadways, traffic control devices, and routes) and vehicular data (volumes, traffic composition, and speed distribution) to produce a graphically animated transportation system. The graphically animated transportation system approximates network performance data under various conditions, including vehicle-miles of travel, vehicle-hours of travel, speed, density, and throughput statistics.

Parameters of the simulation model were calibrated for the JFX corridor by iteratively comparing output of the models with observed driving behavior; adjustments were made as needed to reasonably replicate the observed condition. A simulation model deemed calibrated can reasonably replicate actual/observed conditions within acceptable levels of error.

The GEH, a modified chi-squared test, compared the simulated traffic data with traffic counts for the JFX corridor. The differences between the model's simulated throughputs and the observed traffic counts were well within acceptable error margin, indicating that the model adequately simulates the traffic flow pattern in the study area (Table 1).

Table 1: Observed Versus Simulated Throughputs in Study Area

JFX Segment Southbound	Observed Volume (VPH) (O)	Simulated Volume Range (VPH) (E)	GEH $= [(O-E)^2 / 0.5(O+E)]^{0.5}$	Validation Criteria Met? * (GEH < 5)
Between Exit 5 and Exit 4	8075	7595 – 7879	2.20	Yes
Between Exit 4 and Exit 3	7120	7434 – 7731	3.68	Yes
Between Exit 3 and Exit 2	5886	5979 – 6184	1.21	Yes
Between Exit 2 and Exit 1	5712	5141 – 5497	2.87	Yes
Southbound Right onto Fayette Street	1429	1284 – 1428	0.00	Yes
Southbound through onto President Street	2673	2097 – 2336	6.73	No
Southbound Left onto Fayette Street	1610	1392 - 1592	0.45	Yes

Note: A GEH of between 5 and 10 does not indicate that the model is a poor fit, but that further investigation is required.

Monte Carlo Simulation

The Monte Carlo simulation was used with VISSIM simulation software to find the relationship between post-incident recovery time, traffic intensity, and incident duration. Traffic and incidents were simulated under normal operating conditions to determine the temporal traffic-flow data on the freeway for pre- and post-incident periods (Figure 3).

The simulated freeway segment is a 10-mile, three-lane, unidirectional straight section with no off-ramps, on-ramps, lane drops, grades, or any other bottlenecks (Figure 4). We simulated traffic and incident conditions along the freeway for 150 minutes (2.5 hours). Figure 5 shows a typical time-speed-density graph of simulated incidents and traffic recovery. We then created different scenarios by testing various timed incident durations and traffic intensity levels (volume to capacity). The simulation involved 121 scenarios of traffic intensity (Rho) and incident duration, resulting in 726 experiments. From these 726 experiments, values for output flow, density, speed, and traffic recovery times were derived. The experiments covered various lane-blockage scenarios for the three-lane freeway segment. To suggest an incident that resulted in three lanes being blocked, traffic signals were activated on all three lanes of the freeway segment. For a two-lane blockage, traffic signals were activated on two lanes. To simulate an incident that blocked one lane, one traffic signal was activated on one lane.

Figure 3: Conceptual Layout of Simulation Process
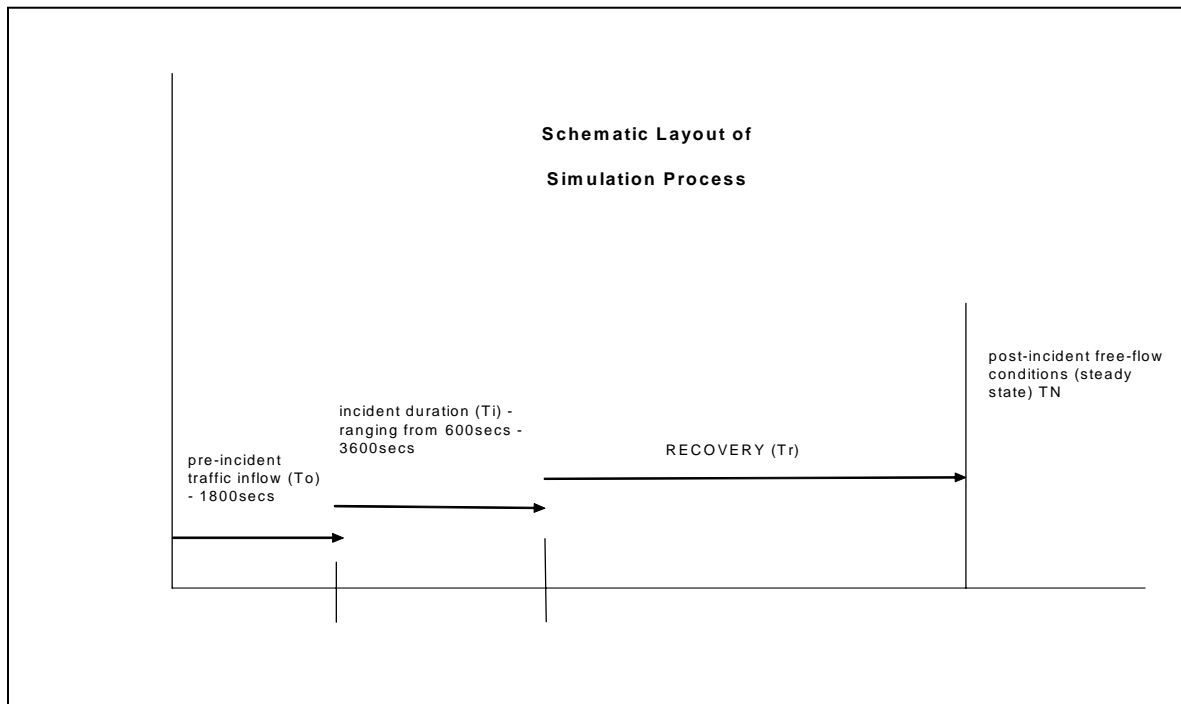
Figure 4: Incident Layout on Freeway[1] (Typical Three-Lane Unidirectional)

Traffic enters freeway on all lanes 30 minutes prior to start of incident

10-Mile freeway

Traffic signals set approximately 7 miles from start of freeway segment

Incident created by traffic signal and activated for incident duration on each lane.

---
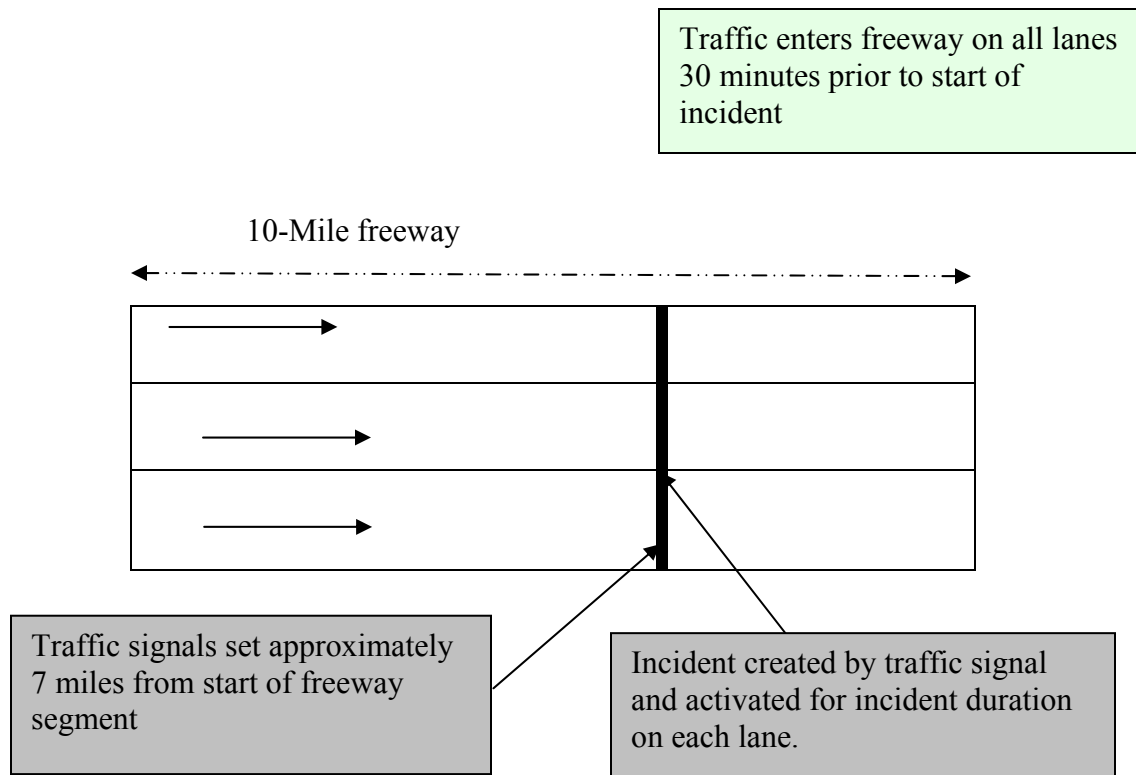
[1] Hobeika and Dhulipala (2004)

Figure 5: Typical Time-Speed-Density Graph of Simulated Incidents and Traffic Recovery
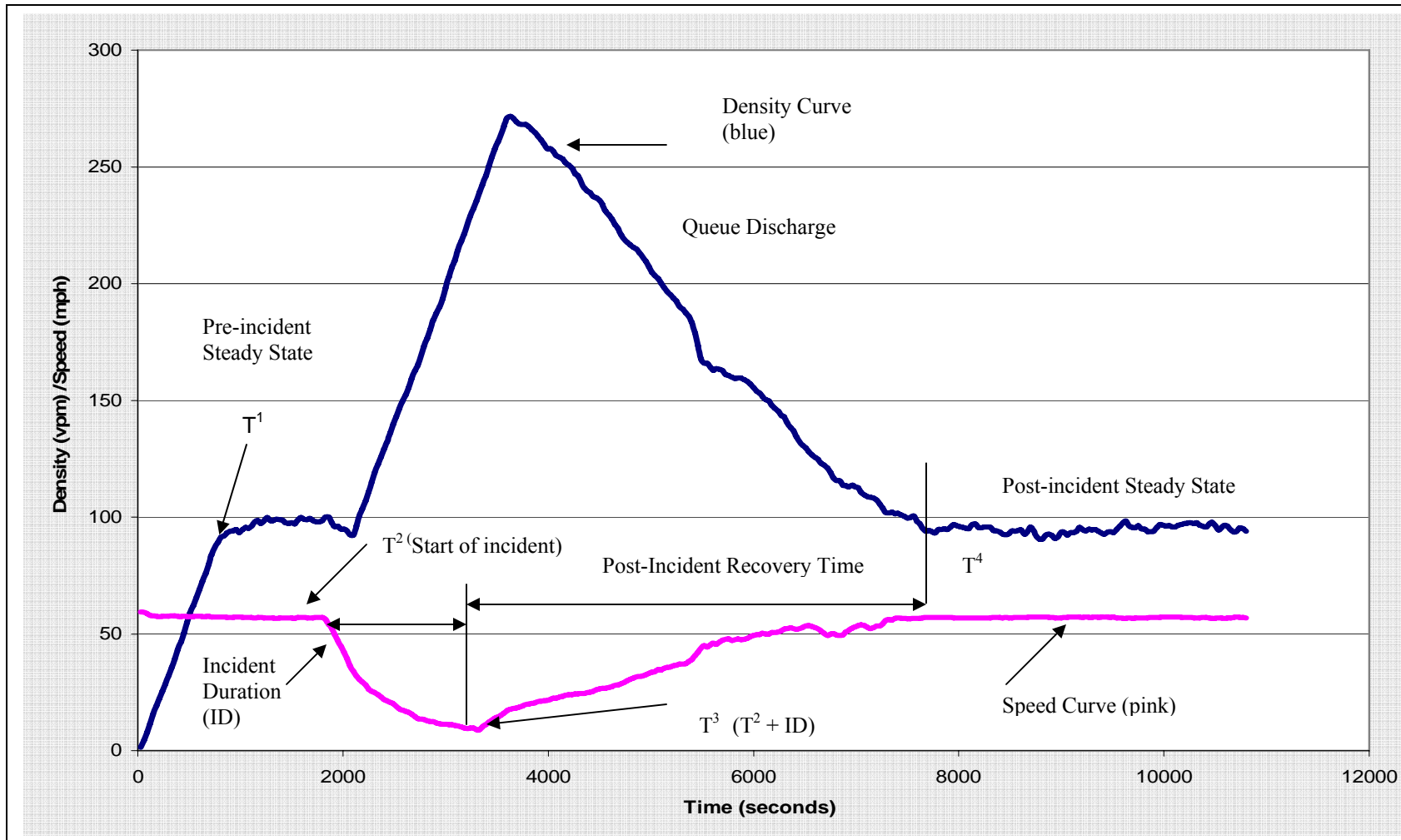
Freeway Capacity

To determine the capacity of the freeway, traffic conditions were simulated along the three-lane, 10-mile section for different flow thresholds, and the resulting throughput (output flow) were compared. Freeway capacity was defined as the point at which the throughput remained unchanged or declined even as the input flow continually increased. As such, freeway capacity for the study was determined to be 2400 vehicles per hour per lane (vphpl). The time-speed-density graphs in Figures 6-13 present some of these simulation results. Incident time ranged from a low of 5 minutes to a maximum of 60 minutes, with incident duration increasing in 5-minute intervals.

Traffic Flow (Demand)

Table 2 presents details on the lane and simulation volumes across different *Rho* (*v/c*). The volumes for the freeway at/near capacity (*Rho* 1.0, 0.95 and 0.90) were 2400 vphpl, 2280 vphpl and 2160 vphpl respectively. The volumes for moderate *Rho* 0.5 and 0.75 were 1200 vphpl and 1800 vphpl, and the volume for light traffic *Rho* 0.25 was 600 vphpl. The simulation run time for each scenario was 150 minutes (2.5 hrs). Under basic freeway operational guidelines, traffic was allowed on all lanes of the freeway for 30 minutes prior to the incident.

Table 2: Volumes and Traffic Intensity at Simulation Start: Three Lanes Blocked

Initial Traffic Intensity (Rho)*	Volume (vphpl)**	3-lane Volume (vph)***	Demand for 2.5 hour of Simulation
1.00	2400	7200	18,000
0.95	2280	6840	17,100
0.90	2160	6480	16,200
0.85	2040	6120	15,300
0.80	1920	5760	14,400
0.75	1800	5400	13,500
0.70	1680	5040	12,600
0.65	1560	4680	11,700
0.60	1440	4320	10,800
0.50	1200	3600	9,000
0.35	840	2520	6,300
0.25	600	1800	4,500

Rho – expressed as a ratio of volume to capacity (v/c). Determines the traffic intensity and is defined as arrival rate to service rate.
*** vphpl – vehicle per hour per lane*
**** vph – vehicle per hour*

Traffic Intensity

Traffic intensity was categorized as light ($0.25 \leq Rho \leq 0.5$), moderate ($0.5 < Rho \leq 0.80$), or near capacity ($0.8 < Rho < 1.0$). Incident scenarios were then generated across these three traffic intensity levels.

Random Seeds

Different combinations of incident duration, effective flow input, and traffic intensity were generated for six different random seeds to derive post-incident values for flow, density, speed and time. The Common Random Number (CRN) variance reduction method (VRN)[2] was used in the Monte Carlo experiment to minimize the variance of the output random variable (e.g. speed, density, and flow) across the different traffic scenarios considered.

Effective *Rho* [ρ^1] – Definition and Calculation (Three-Lane)

Actual simulations for each three-lane scenario were determined based on the calculated effective *Rho* (see Appendix 2). The scenarios were not simulated if the calculated effective Rho [ρ^1] was greater than one because any value greater than one suggests that there would be no reasonable recovery, as the recovery would be indefinite. The effective *Rho* value for each scenario (traffic intensity and incident duration) is derived as a ratio of total demand for the simulation period to effective capacity for the specified incident duration. Total demand is calculated for the simulation period at the specified traffic intensity or initial *Rho* value. Effective capacity is defined as the potential throughput for the simulation period (total supply) less the unmet demand for the incident duration at the specified traffic intensity level or original *Rho* value. Potential throughput (18,000 vehicles) is the capacity of the unidirectional three-lane freeway for the entire 150 minute simulation period.

The traffic intensity (*Rho* value) would be higher when an incident happens resulting in a lower capacity. We define this traffic intensity as effective *Rho* which is calculated below.

Equation 1: Calculation of Effective *Rho* [ρ^1]

$$Rho^1 = \frac{\text{Total Volume for the Simulation Time}}{\text{Effective Capacity for Incident Duration}} = \frac{T_S * Rho * C * L}{T_S * C * L - T_I * L * C * rho}$$

---

[2] Law and Kelton

Where:

T_S = Simulation period = 9000 sec

C = Capacity = 2400 $vphpl$

V = Volume

Rho = V/C ∈ [0.25 − 0.95]

L = Total number of lanes ∈ {1,2,3}

T_I = Incident time ∈ {5,10,15,...,50,55,60}

Rho^1 = Effective Rho

Calculation of Effective *Rho* Values (e.g. *Rho* = 0.9)

- Total potential throughput (supply) capacity for simulation period = 3*2400*2.5hrs (9000sec) = 18,000

- Total (demand) volume for 9000 sec simulation = 2.5*(0.9*2400*3) = 16,200

- With a 30-min incident, for a 90 percent throughput, unmet demand = 0.9*(7200*30/60) = 3240

- Effective capacity for incident duration of 30 mins = 18,000 - 3240 = 14,760

- Effective *Rho* for 30-min incident = 16,200/14,760 = 1.10

Appendix 2 presents the deterministically calculated effective *Rho* [ρ^1] values for the case of all three lanes closed. In the case of only one or two lanes closed, we used simulation in estimating (Equation 2) the ensuing effective *Rho* [ρ^2] because of the complexity posed by lane-change/merge activities and the associated stochastic effects on the throughput.

Equation 2: Calculation of New Effective *Rho* [ρ^2]

$$Rho^2 = \frac{\text{Total Volume for the Simulation Time}}{\text{Effective Capacity for Incident Duration}} = \frac{T_S * Rho * C * L}{T_S * C * L - (Qpri - Qid)}$$

Where:

T_S = Simulation period = 9000 sec

C = Capacity = 2400 *vphpl*

V = Volume

Rho = V/C $\in [0.25 - 0.95]$

L = Total number of lanes $\in \{1,2,3\}$

T_I = Incident time $\in \{5,10,15,...,50,55,60\}$

Rho^1 = Effective Rho

$Qpri = Average\_Volume\_preincident$

$Qid = Average\_Volume\_incident\_recovery$

Validation of Recovery Time Determination

As previously mentioned, determination of the post-incident traffic recovery time was based on the pre-incident steady state condition, i.e., the prevailing traffic density and speed. Table 3 presents sampling results of the density data used to validate the recovery-time determination. A systematic sampling technique was used to select the scenarios. The t-test results were statistically significant for all but two blockage scenarios: *Rho* 0.7/50-min (one-lane) and *Rho* 0.8/15-min (two-lane). The t-test confirms no statistically significant difference between pre-incident and post-incident steady state mean for density used in determining the recovery time.

Table 3: Summary Results of t-test for Paired Two Sample

Lane Scenario	Traffic Intensity (*V/C*)	Inc-Duration (min)	Pre-Incident Means	Post-Incident Means	*N*	t- Stat	P(*T<=t*)	T Critical
Three	**0.9**	**10**	116	117	6	-0.227	0.829	2.571
Lanes	**0.8**	**15**	103	103	6	0.095	0.928	2.571
Blocked	**0.8**	**30**	106	102	4	1.367	0.265	3.182
	0.7	**50**	91	88	3	1.389	0.299	2.571
Two	**0.9**	**10**	117	117	6	0.031	0.976	2.571
Lanes	**0.8**	**15**	100	103	6	-3.198	0.024	2.571
Blocked	**0.8**	**30**	101	103	6	-1.310	0.247	2.571
	0.7	**50**	72	89	6	-1.132	0.309	2.571
One	**0.9**	**10**	114	117	6	-2.291	0.071	2.571
Lane	**0.8**	**15**	101	103	6	-1.831	0.127	2.571
Blocked	**0.8**	**30**	101	102	6	-0.873	0.422	2.571
	0.7	**50**	85	89	6	-2.999	0.030	2.571

RESULTS AND ANALYSIS

Time-Speed-Density Graphs - Scenario 1: Three Lanes Blocked

The following time-speed-density graphs show three segments of the time-speed and time-density graphs (un-congested, congested, and queue discharge), and the simulation results for incident durations of 5, 25, and 45 minutes. As expected, the graphs confirm that for the same incident duration, post-incident recovery time is higher at traffic intensity levels at or near capacity than for moderate to low traffic intensity levels. A brief examination of the time-speed-density graphs for the 5-minute and 25-minute incidents time shows that the recovery time increases proportionately with the increase in *Rho* values on both incident duration times. The queue discharge for *Rho* 0.60, 0.85 and 0.95 is much longer at each incident duration time than for the lower *Rho* values of 0.25, 0.35 and 0.50.

Figure 6: 5-Min Simulated[3] Incident – *Rho* 0.65: Three Lanes Blocked

---
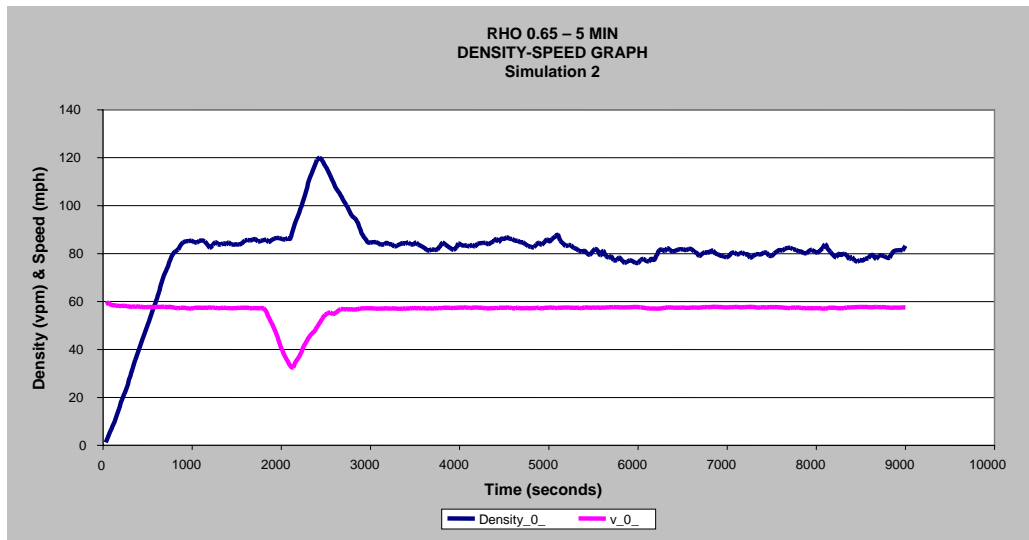
[3] "Density_o_": density in vehicles per mile (vpm); "V_o_" speed in miles per hour (mph)

Figure 7: 5-Min Simulated Incident – Rho 0.95: Three Lanes Blocked
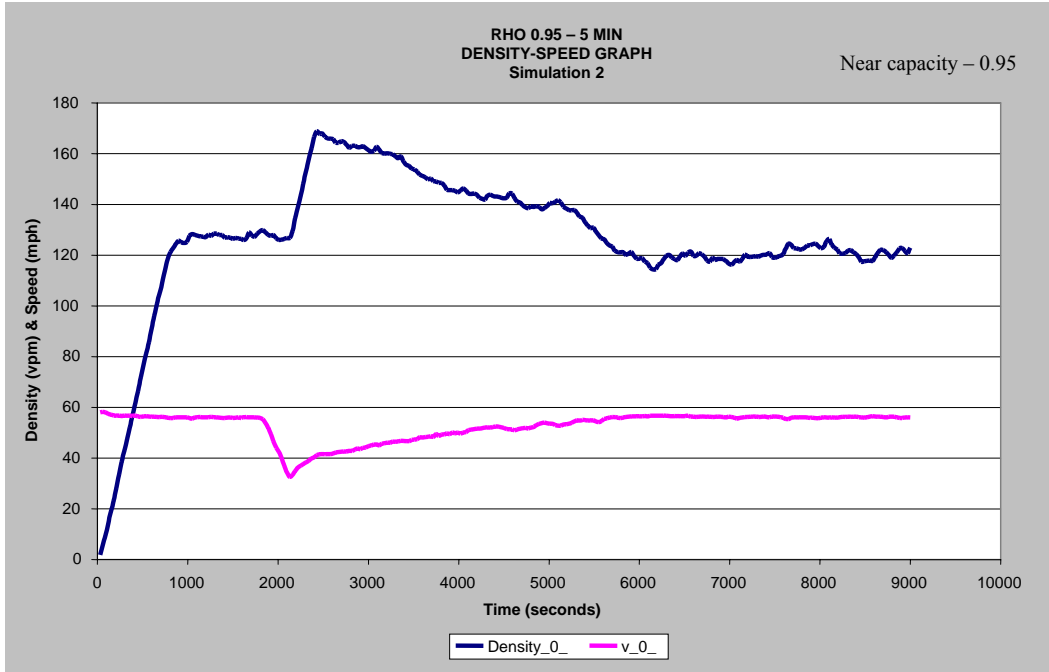
Incident time = 5 min
Rho= 0.65, recovery time = 945 sec (16 min)
Rho= 0.95, recovery time= 4495 sec (75 min)

Figure 8: 25-Min Simulated Incident – *Rho* 0.35: Three Lanes Blocked

24
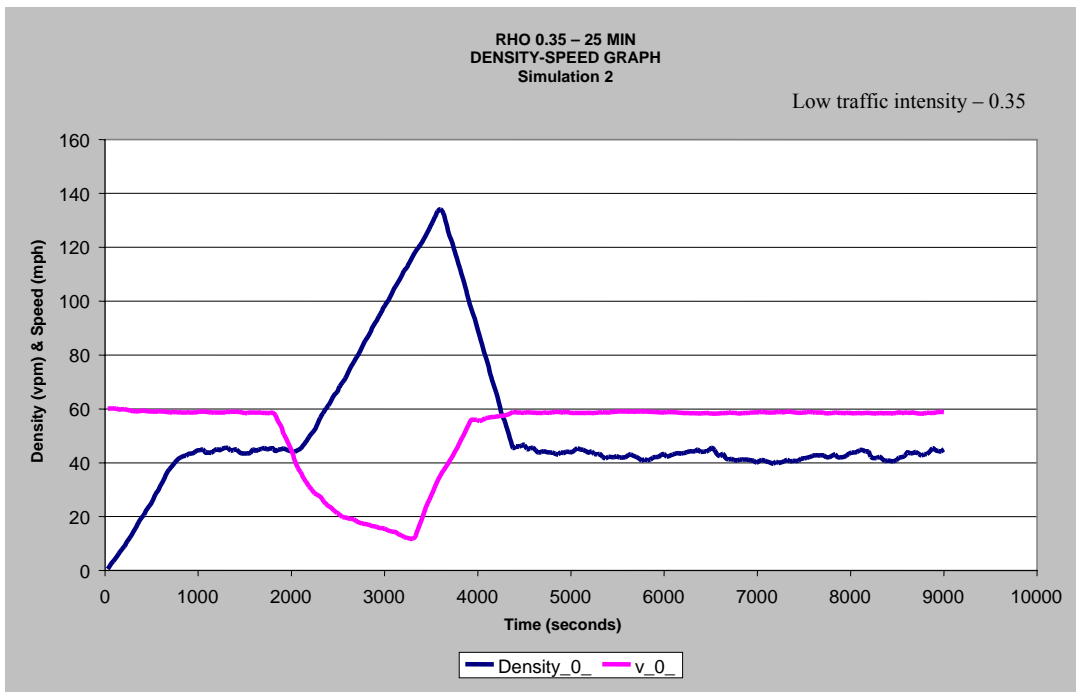
Figure 9: 25-Min Simulated Incident – *Rho* 0.60: Three Lanes Blocked
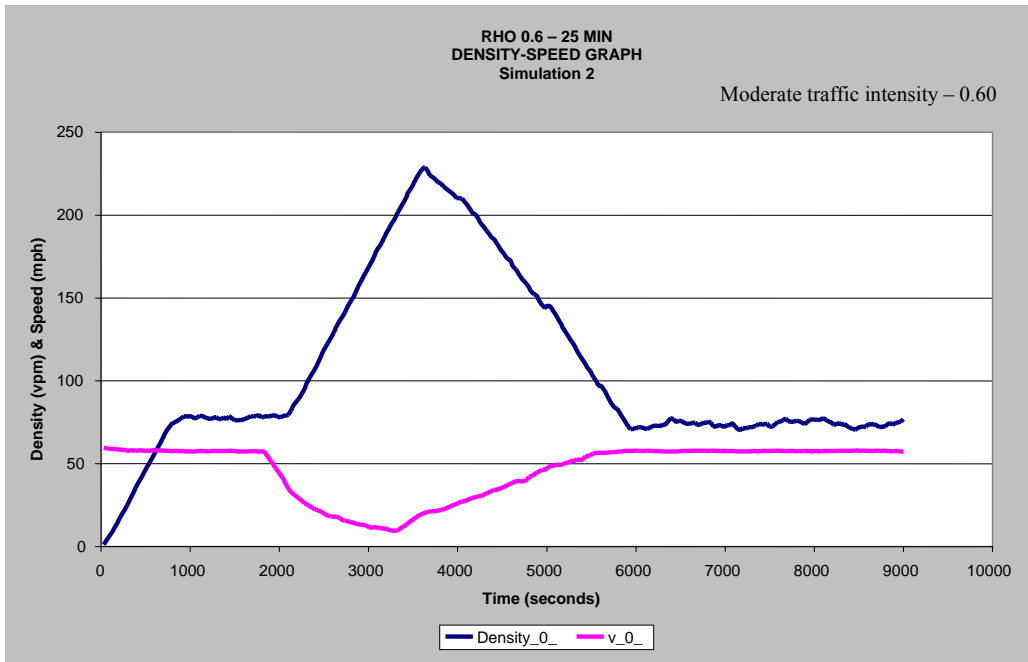
Incident time = 25 min
Rho=0.35, recovery time= 1350 sec (23 min)
Rho= 0.60, recovery time= 2575 sec (43 min)
Rho=0.85, recovery time= inconclusive

Figure 10: 25-Min Simulated Incident – *Rho* 0.85: Three Lanes Blocked
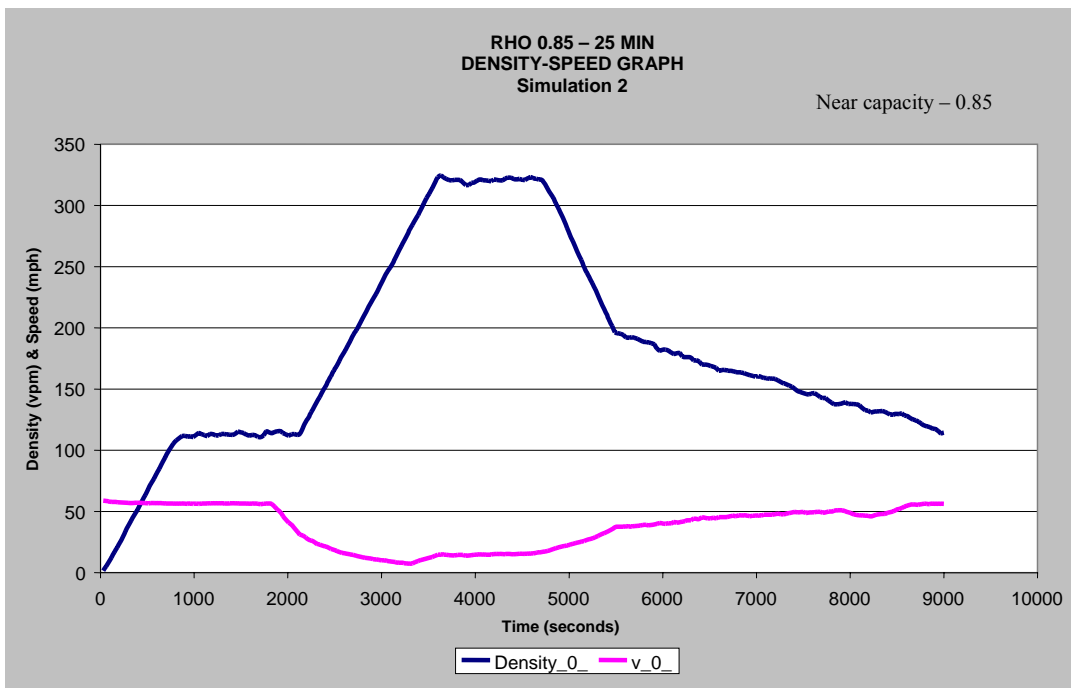
Figure 11: 45-Min Simulated Incident – Rho 0.25: Three Lanes Blocked

RHO 0.25 – 45 MIN
DENSITY-SPEED GRAPH
Simulation 2

Low traffic intensity – 0.25
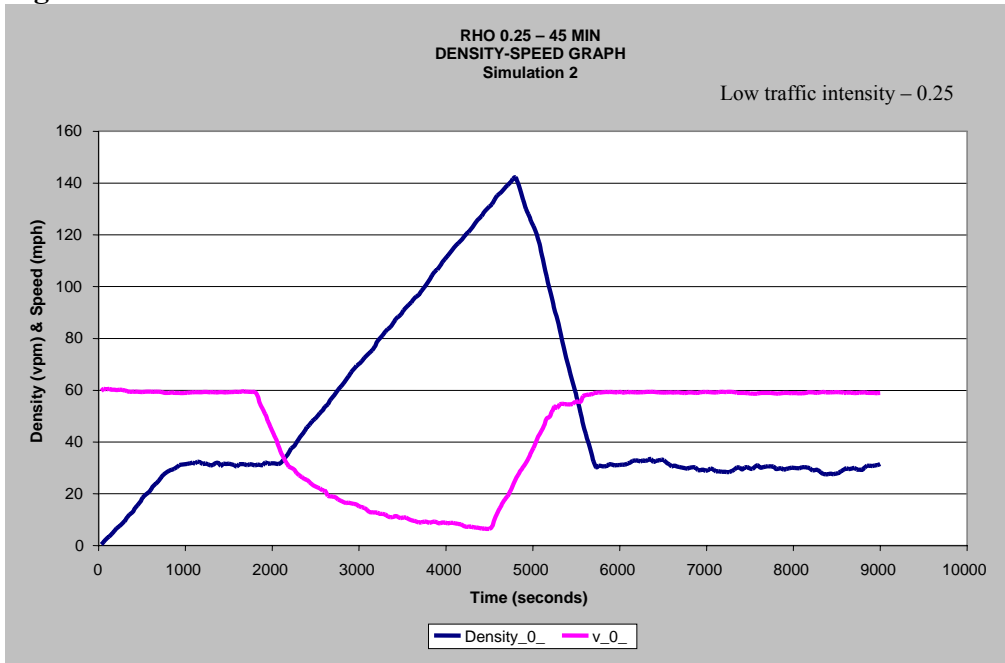
Incident time = 45 min
Rho=0.25, recovery time= 1285 sec (22 min)
Rho=0.50, recovery time= 3015 sec (50 min)
Rho=0.75, recovery time= inconclusive

Figure 12: 45-Min Simulated Incident – *Rho* 0.50: Three Lanes Blocked

RHO 0.5 - 45 MIN
DENISTY-SPEED GRAPH
Simulation 2

Moderate traffic intensity – 0.50

26
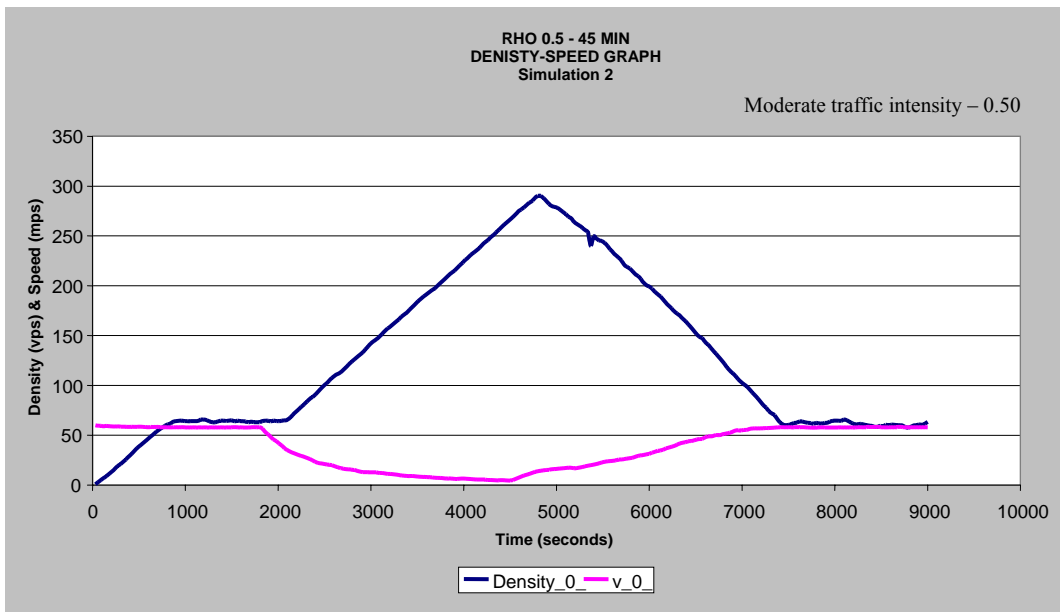
Figure 13: 45-Min Simulated Incident – *Rho* 0.75: Three Lanes Blocked
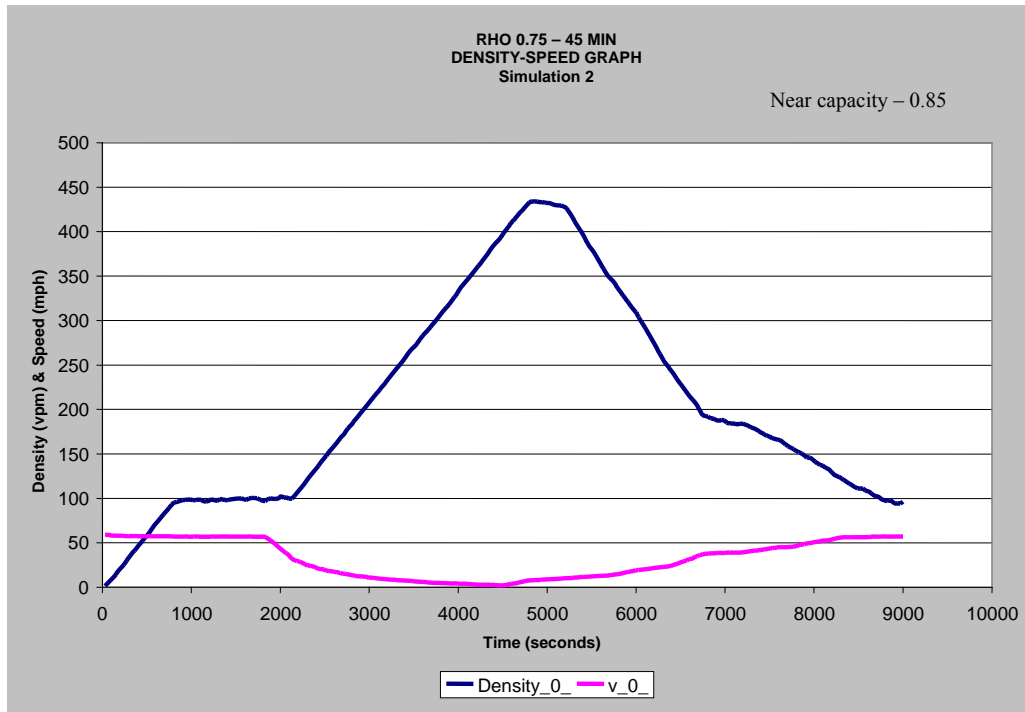
Simulation Summary Results - Scenario 1: Three Lane Blocked

Table 4 shows a spreadsheet with the summary results for 97 scenarios of six random number seeds for each combination of traffic intensity and incident duration. A total of 582 experiments were generated on the three-lane blockage scenario. Post-incident traffic recovery values for 18 scenarios were inconclusive and not included in the analysis. These were primarily results for moderate to high (0.60-0.85) traffic intensity with incident durations greater than 25 minutes. In addition, post-incident recovery time was inconclusive for traffic intensity levels of *Rho* 0.60-0.75 at incident durations beyond 45 minutes.

Within the same incident duration, recovery time increases proportionally (nonlinearly) as traffic intensity builds. As traffic intensity approaches the capacity threshold (i.e. *Rho* $[\rho^0] = 1$), recovery time becomes indefinite. However, it must not be assumed that recovery time always increases with incident duration. At low to moderate traffic intensity levels for scenarios involving partial blockage (one or two lanes blocked), recovery time begins to stabilize beyond certain incident duration. This condition likely occurs as traffic upstream of the incident begins to change to unblocked lanes and eventually achieves a steady state in a different flow regime.

The experiments performed showed post-incident recovery time ranged from a high of 93 minutes (for a traffic intensity of 0.9 and 15-minute incident duration), to a low of 9 minutes (for traffic intensity of 0.25 and a 5-minute incident).

27

Table 4: Post-Incident Traffic Recovery Time: Three Lanes Blocked

Original Rho ρ^0	Incident Time (minutes)											
	5	10	15	20	25	30	35	40	45	50	55	60
0.25	9	12	16	15	16	17	18	20	21	23	25	26
0.35	12	16	15	21	23	27	28	30	32	35	38	40
0.50	15	19	24	29	35	38	42	46	50	55	58	60
0.60	15	21	28	36	43	51	60	67	69	**	**	**
0.65	16	26	35	43	51	64	68	74	**	**	**	**
0.70	23	34	49	57	70	77	79	**	**	**	**	**
0.75	21	35	51	62	76	**	81	**	**			
0.80	36	49	60	77	89	**	**					
0.85	37	58	78	90	**							
0.90	62	86	93									
0.95	75											

NB: Post-Incident Traffic Recovery - is calculated as the time (T^4) at start of steady state post-incident recovery less time (T^3) at the end of the incident. See Figure 5.
** Post-Incident Traffic Recovery times omitted, as they were inconclusive.

Table 4 shows *Rho* 0.25 returns the lowest post-incident recovery time of 9 minutes for a 5-minute incident, followed by *Rho* 0.35 with 12 minutes. At *Rho* of 0.25, the post-incident recovery time (26 minutes) for a 60-minute incident duration is less than that for *Rho* 0.5 for a 20-minute incident (29 minutes) and *Rho* 0.75 for 10-minute incident duration (35 minutes). Similarly, for *Rho* 0.5 and 60-minute incident duration, the traffic recovery time (60 minutes) is about the same as that for a 20-minute incident at *Rho* of 0.75 (62 minutes). Simulation results indicate that congestion increases as incident duration increases at all *Rho* values but increases at faster rates for higher *Rho* values. Figure 14 is a graphical depiction of the summary results for three-lane blocked scenarios.

Table 5 shows a sample of the post-incident recovery times and the comparisons across different scenarios of traffic intensity and incident durations. Note that maximum simulated recovery time (> 85 minutes) occurs for traffic intensity levels near capacity (0.85-0.90) but across incident durations ranging from 10-20 minutes. Post-incident recovery times from 74-79 minutes occur across traffic intensity levels ranging from moderate to near capacity. Recovery times between 74-79 minutes occur across decreasing *Rho* values with increasing incident times (0.95-5 minutes, 0.85-15 minutes,

0.80-20 minutes, 0.70-25 minutes, 0.70-30 minutes). Post-incident recovery times between 67-69 minutes are concentrated within moderate traffic intensity levels (0.60-0.75) with incident durations ranging from 35-45 minutes. Figures 15-17 present traffic recovery as a function of traffic intensity across the same incident durations.

Figure 14: Post-Incident Recovery Time: Three Lanes Blocked
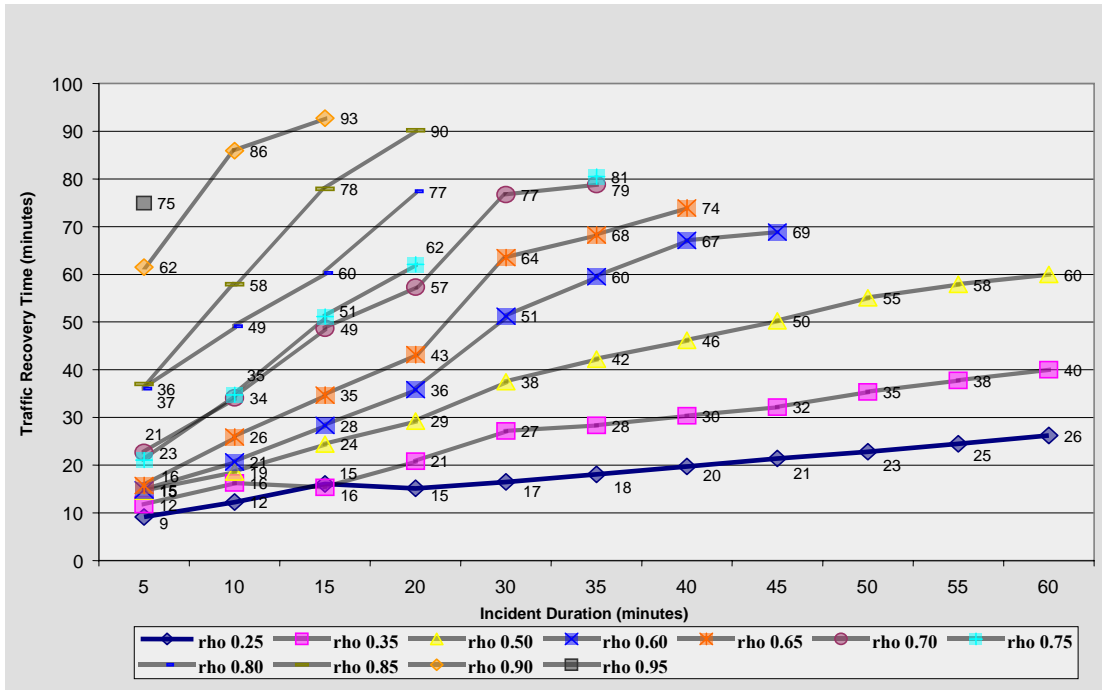
Figure 15: Post-Incident Recovery as a Function of *Rho*: 5-Min Incident

29
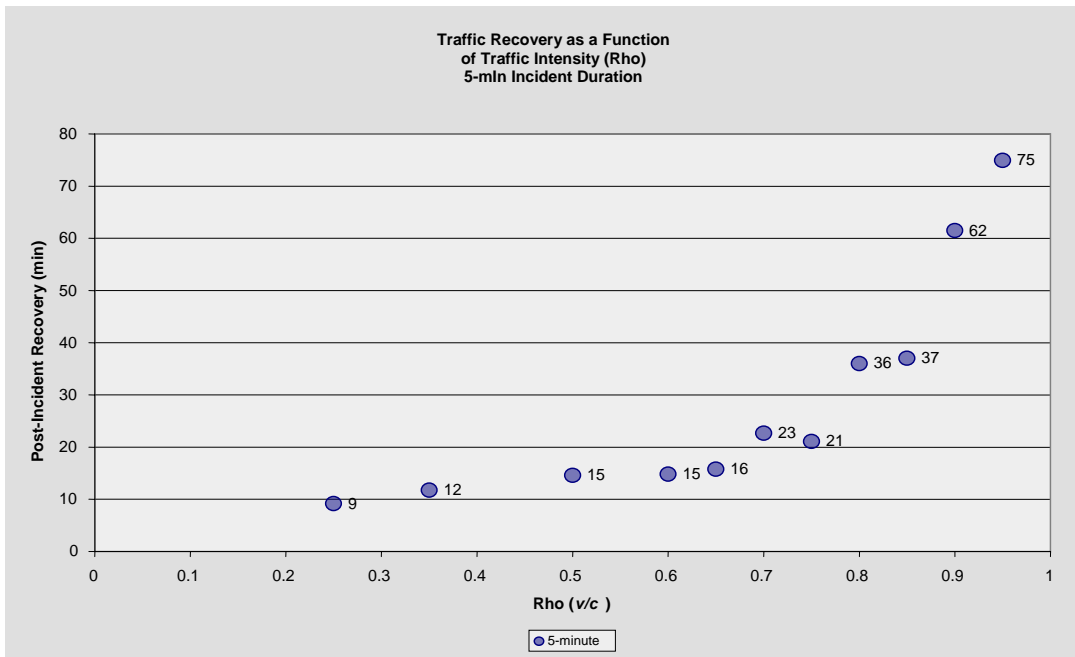
Table 5: Comparison of Post Incident Recovery Times — Three Lanes Blocked

Post-Incident Recovery Time (min)	Post-Incident Recovery Time (sec)	Traffic Intensity Original *Rho* (v/c)	Incident Duration (min)
86-93	5155-5565	0.90	10 - 15
		0.85	20
74-79	4434-4728	0.95	5
		0.85	15
		0.80	20
		0.70	30-35
		0.65	40
67-69	4025-4133	0.65	35
		0.60	40-45
60-64	3600-3810	0.90	5
		0.80	15
		0.75	20
		0.65	30
		0.60	30
		0.50	60
55-58	3305-3474	0.85	10
		0.70	20
		0.50	50-55
50-52	3015-3075	0.75	15
		0.6	30
		0.5	45
42-49	2535-2945	0.80	10
		0.70	15
		0.65	20
		0.50	35-40
34-38	2045-2265	0.85/0.80	5
		0.75/0.70	10
		0.65	15
		0.60	20
		0.50	30
		0.35	50-55

Figure 16: Post-Incident Recovery as a Function of *Rho*: 15-Min Incident

Traffic Recovery as a Function
of Traffic Intensity (Rho)
15-min Incident Duration
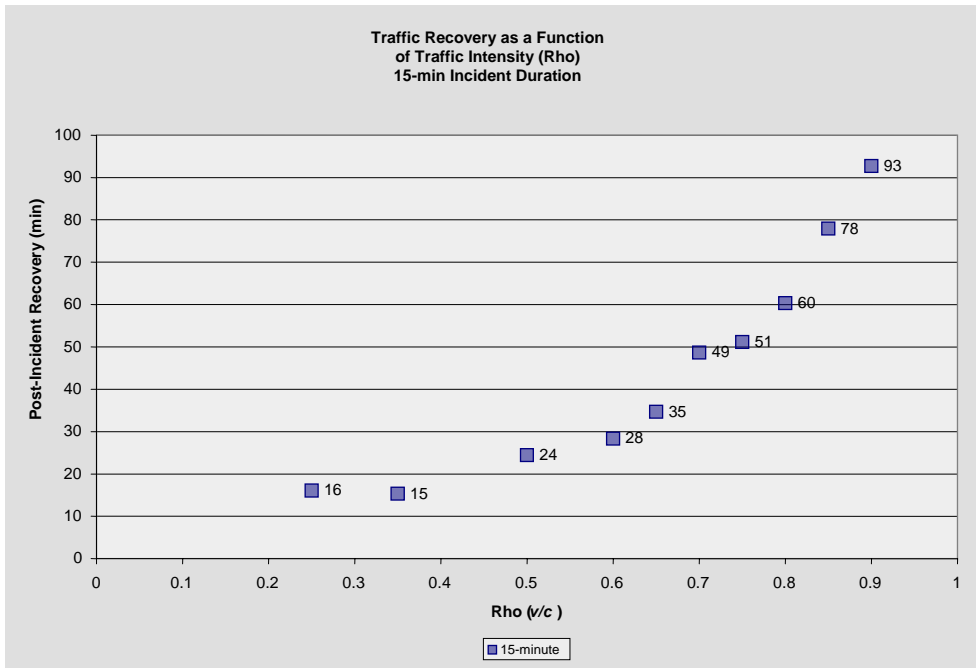
Figure 17: Post-Incident Recovery as a Function of *Rho*: 25-Min Incident

Traffic Recovery as a Function
of Traffic Intensity (Rho)
25-min Incident Duration
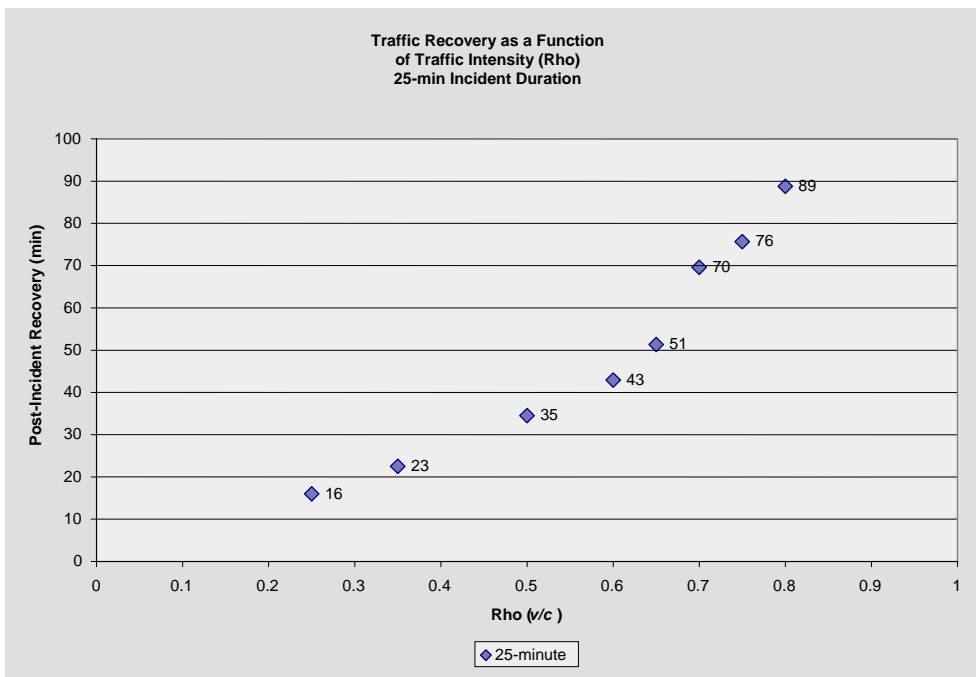
Lane Closure Scenarios

By running simulations for the different lane-closure scenarios (three lanes blocked, two lanes blocked, and one lane blocked), we were able to compare traffic recovery time based on traffic intensity, capacity, and incident time. The three-lane-blockage scenario generated incident occurrences across all traffic intensity levels for 97 scenarios (see Appendix 2). However, for the two-lane and one-lane scenarios, 12 different scenarios of traffic intensity and incident duration were generated primarily on moderate to high traffic intensity levels. Low traffic intensity and incident duration combinations resulted in little or no variations in the traffic recovery times for partial lane blockage scenarios. Consequently, relatively fewer scenarios (12 different scenarios) were analyzed *vis-à-vis* the three-lane blockage scenarios.

Table 6 shows a sampling of the post-incident recovery times across different lane-blockage scenarios. The results across the lane scenarios were consistent at similar traffic intensity levels and incident times. For the same incident time and *Rho* levels, recovery time increases as the proportion of lane blockage increases. In addition, within the same incident duration, recovery times increase proportionally as traffic intensity builds.

Table 6: Comparison of Traffic Recovery Times Across Lane-Blockage Scenarios

Simulation Scenario		Scenario #1 Three Lanes Blocked	Scenario #2 Two Lanes Blocked	Scenario #3 One Lane Blocked
Incident Time	Original *Rho* ρ^0	Recovery Time	Recovery Time	Recovery Time
10MIN	0.90	86	57	28
15MIN	*0.90*	*93*	*74*	*42*
15MIN	0.85	78	52	26
15MIN	0.80	60	44	17
15MIN	0.75	51	35	16
15MIN	0.70	49	31	11
30MIN	0.80	85	62	22
30MIN	0.75	71	54	19
45MIN	0.75	72	68	33
50MIN	*0.70*	*65*	*60*	*26*
55MIN	0.65	64	53	30
60MIN	0.70	**	60	32

** Post-Incident recovery times were omitted, as they were inconclusive.

Table 7 compares original Rho and new effective Rho (derived from simulation) across the lane-blockage scenarios. The original Rho $[\rho^0]$ values are based on freeway capacity volumes whereas the new effective Rho $[\rho^2]$ values are derived from the simulations (see Equation 2).

Table 7: Comparison of Effective *Rho* $[\rho^2]$ Values Across Lane-Blockage Scenarios

Simulation Scenario		Scenario #1 Three Lanes Blocked	Scenario #2 Two Lanes Blocked	Scenario #3 One Lane Blocked
Incident Time	Original *Rho* ρ^0	New Effective *Rho* ρ^2	New Effective *Rho* ρ^2	New Effective *Rho* ρ^2
10MIN	0.90	0.90	0.90	0.90
15MIN	0.90	0.91	0.90	0.90
15MIN	0.85	0.85	0.85	0.85
15MIN	0.80	0.80	0.80	0.80
15MIN	0.75	0.75	0.75	0.75
15MIN	0.70	0.70	0.70	0.70
30MIN	0.80	0.82	0.80	0.80
30MIN	0.75	0.75	0.75	0.75
45MIN	0.75	0.79	0.76	0.75
50MIN	0.70	0.74	0.70	0.70
55MIN	0.65	0.68	0.65	0.65
60MIN	0.70	**	0.71	0.70

** Effective Rho values omitted, as they were inconclusive.

Time-Speed-Density Graphs – Comparison of All Lane Closure Scenarios

Figures 18-20 show *time-speed-density* graphs for simulations across lane closure scenarios for a 15-minute incident. Initial traffic intensity is 0.9. As expected, the recovery time incrementally increases as the number of lane closures increases from one to three lanes.

Density (vehicles per mile) also increases incrementally from one lane closure to three lane closure. Density peaks at around 250 vpm (lanes combined) for a three-lane blockage, 200 vpm for a two-lane blockage, and 140 vpm when one lane is blocked.

Figure 18: Lane Closure Scenarios — 0.9-15 Min: Three Lanes Blocked (Near Capacity)
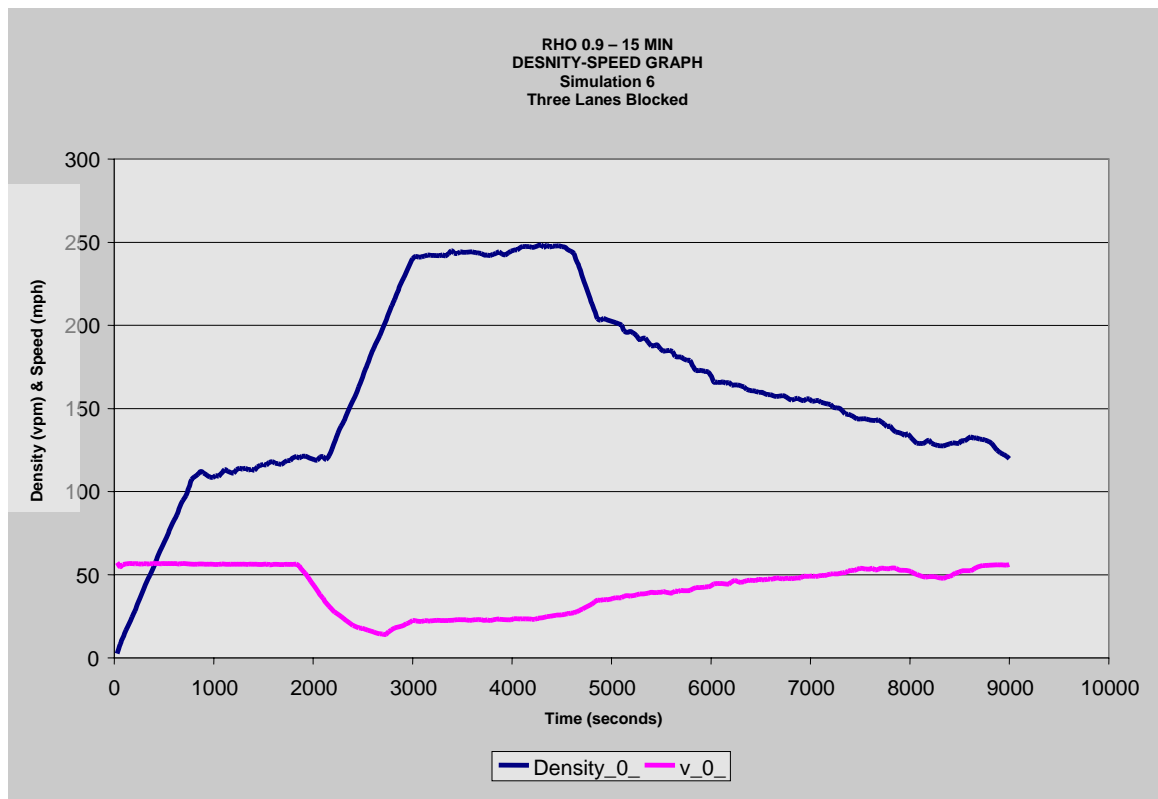
Figure 19: Lane Closure Scenarios — 0.9-15 Min: Two Lanes Blocked (Near Capacity)

RHO 0.90 – 15 MIN
DENSITY-SPEED GRAPH
Simulation 6
Two Lanes Blocked
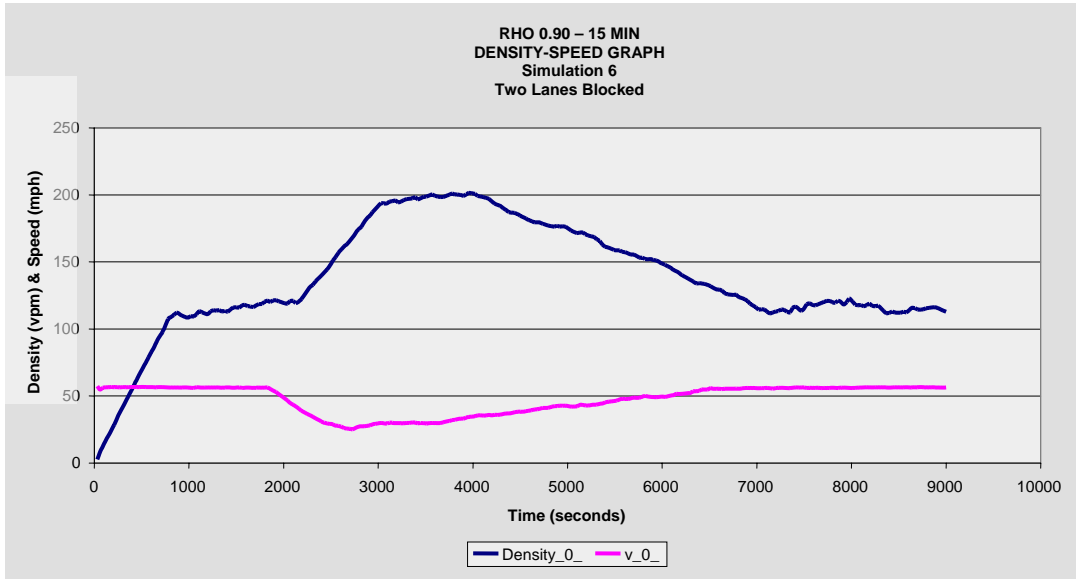
Figure 20: Lane Closure Scenarios — 0.9-15 Min: One Lane Blocked (Near Capacity)

RHO 0.90 – 15 MIN
DENSITY-SPEED GRAPH
Simulation 6
One Lane Blocked
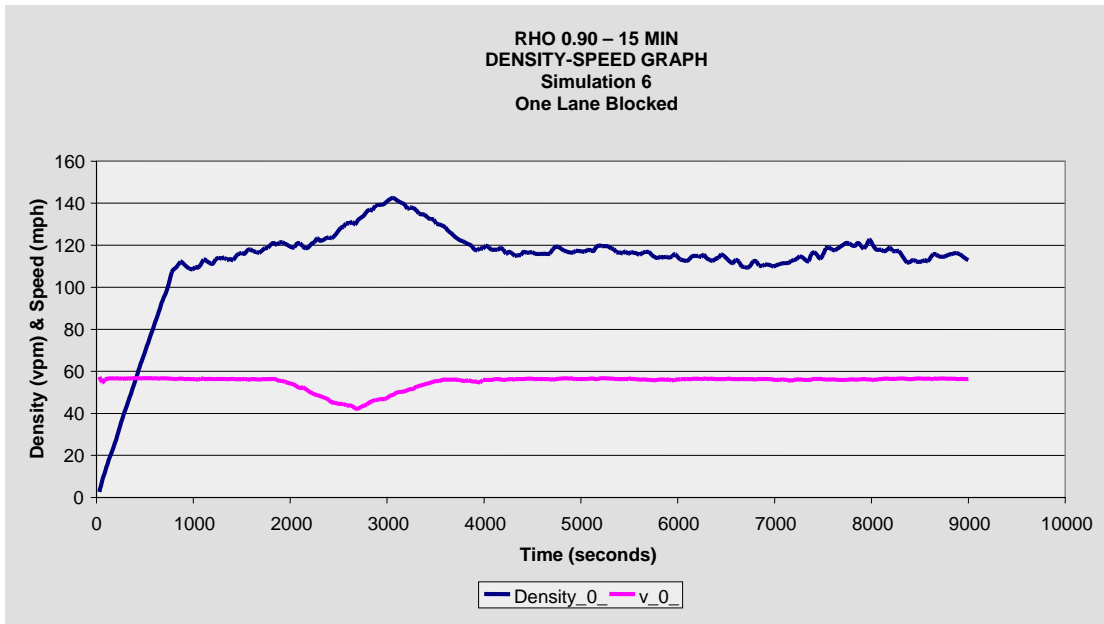
Figure 21: Lane Closure Scenarios — 0.7- 50 Min: Three Lanes Blocked (Moderate Intensity)
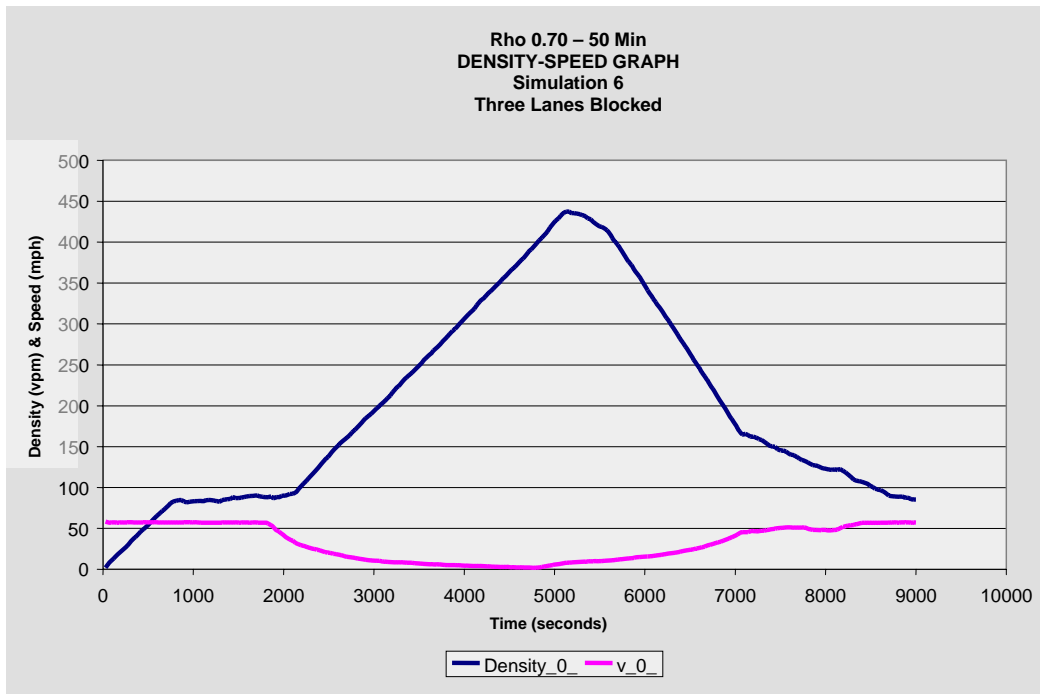
Figures 21-23 show *time-speed-density* graphs for simulations of a 50-minute incident across all lane closure scenarios with an initial traffic intensity of 0.7. The recovery time increases incrementally as the number of closures increases from one to three lanes.

Density (vehicles per mile) also increases from one lane closure to three. Density peaks at around 430 vpm (lanes combined) for three blocked lanes, 270 vpm for two blocked lanes, and 90 vpm for one blocked lane.

When comparing recovery times for these two different traffic intensity levels, note that although the incident time at traffic intensity of 0.7 is 50 minutes, the post-incident recovery times are significantly lower than for traffic intensity at 0.9 for 15 minutes. This result is consistent for other similar intensity-duration scenarios.

This suggests that traffic intensity, rather than incident duration, may be a stronger indicator of recovery times.

Figure 22: Lane Closure Scenarios — 0.7- 50 Min: Two-Lanes Blocked (Moderate Intensity)

RHO 0.70- 50MIN
DENSITY-SPEED GRAPH
Simulation 6
Two Lanes Blocked
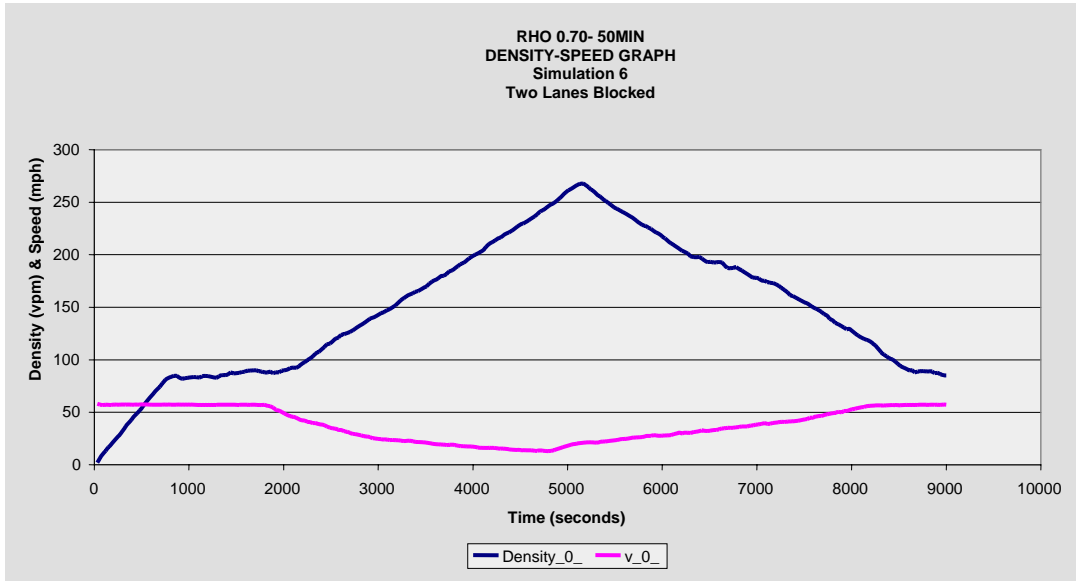
Figure 23: Lane Closure Scenarios — 0.7- 50 Min: One-Lane Blocked (Moderate Intensity)

RHO 0.70 - 50 MIN
DENSITY-SPEED GRAPH
Simulation 6
One Lane Blocked
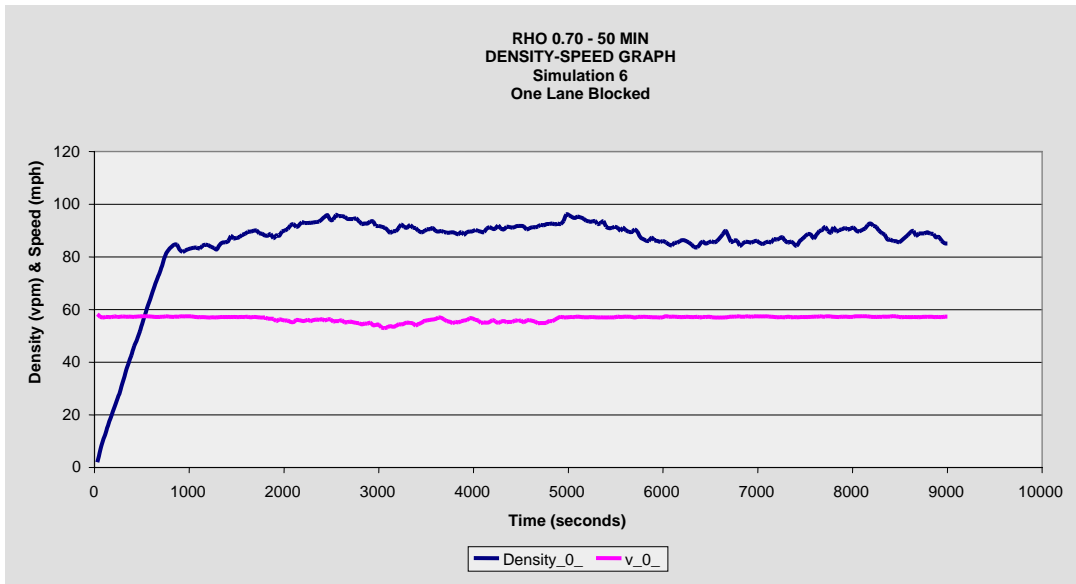
REGRESSION ANALYSIS

Simulation results were processed to calculate traffic recovery time, which is defined as the time after clearance of an incident for traffic flow to return to normal or steady state. The average of the six recovery times for each combination of incident time and *Rho* values for all lane-blockage scenarios was calculated and can be seen in Appendix 4.

We utilized Model Quest[4], the modeling software, to find the relationship between traffic recovery time (endogenous variable) and incident time and traffic intensity (exogenous variables). With an adjusted R^2 of 0.887 aggregated for all variables, we concluded that traffic recovery time can be reasonably represented as a nonlinear function of incident time and traffic intensity. When the results were grouped based on traffic intensity level — [light ($0.25 \leq Rho \leq 0.5$), moderate ($0.5 < Rho \leq 0.80$), and near capacity ($0.8 < Rho < 1.0$)] — we obtained a better model to estimate the coefficients of this relationship. We explored three different models: (1) nonlinear regression aggregated for all variables, a total of 107; (2) nonlinear regression based on traffic intensity levels and; (3) nonlinear regression for all lane-blockage scenarios.

The nonlinear regression was based on natural log transformation of the simulated recovery times (endogenous variable). Table 8 presents the summary results of the R^2 and adjusted R^2 values for the nonlinear regression models considered.

Table 8: Summary Results of Regression Models

REGRESSION MODELS	R Squared (R^2)	Adjusted R^2	N
AGGREGATED ALL	0.863	0.851	107
TRAFFIC INTENSITY LEVELS:			
Near Capacity(0.8<Rho<1.0)	0.999	0.907	14
Moderate Intensity (0.5<Rho≤ 0.80)	0.996	0.977	57
Low Intensity (0.25≤Rho≤0.5),	0.999	0.968	36
LANE SCENARIOS:			
Three Lanes Blocked	0.989	0.976	83
Two Lanes Blocked	1.000	0.900	12
One Lane Blocked	0.997	0.897	12

---

[4] AbTech Corporation, ModelQuest Version 4.0

As reported, the R^2 is greater than 85 percent in all options and is high enough to explain this log linear relationship. Results for all the regression models are statistically significant at a probability <0.05 for all variables. The regression model comparing across traffic intensity levels returns the highest adjusted R^2 values ranging from 91-98 percent.

Regression All (Aggregated) Results

Equation 2: All Variables - No Intercept

$$\text{Log}_e \, T_R = 2.819 Rho + 0.021 T_i + 1.475 L$$

$$(0.000)^5 \quad (0.000) \quad (0.000)$$

$R^2 = 0.863$

Adjusted $R^2 = 0.851$

$N = 107$

> Where:
> T_R = Recovery time (min)
> L = Proportion of lanes closed
> N = Number of data points
> $Rho = V/C$ [0.25-0.95]
> T_i = Incident Duration [5,10,…60]

The regression model, intercept zero, shows a strong correlation between all the variables with an R^2 of 0.863. The adjusted R^2 suggest that over 85 percent of the variance in post-incident traffic recovery can be explained by the variables traffic intensity (v/c), incident duration and the proportion of lane closure. The results are statistically significant at p<0.005 for both traffic intensity and incident duration. The strongest association was indicated by an R2 of 0.935 for traffic intensity (Rho) with an adjusted R^2 of 0.926, suggesting that traffic intensity accounts for almost 93 percent of the variance in post-incident recovery time. Incident time and lane blockage returned an adjusted R^2 of 0.736 and 0.920 respectively. However, when traffic intensity and incident duration were combined, the R^2 improved to better than 0.975 with an adjusted R^2 of 96 percent (Appendix 9-13). Figure 24 presents the simulated recovery times versus the calculated values from regression for all simulations.

---

[5] The numbers in parenthesis are probabilities for t-values of coefficients. Probability values less than 0.05 are considered significant at the 5 percent level of significance.

Figure 24: Simulated Traffic Recovery Times vs. Regression Values, All Variables

Recovery Time - Regression vs. Simulation
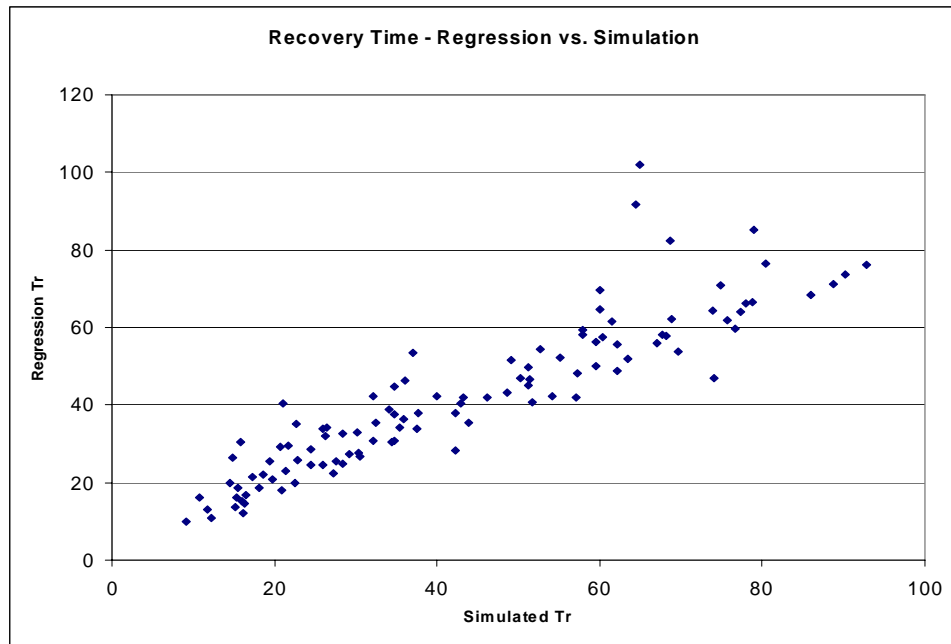
Regression – Traffic Intensity Scenarios

Nonlinear regression analysis was also performed for the three traffic intensity scenarios: light ($0.25 \leq Rho \leq 0.5$), moderate ($0.5 < Rho \leq 0.80$), and near capacity ($0.8 < Rho < 1.0$). Equations 4-6 summarize the results. The R^2 value for all scenarios is extremely high and indicates a strong correlation between the post-incident recovery time and the variables for traffic intensity, incident duration, and proportion of lane blockage. The moderate traffic intensity scenario had the lowest reported R^2 value of 0.996, with 0.999 for both near capacity and low traffic intensity scenarios. The results for each scenario are statistically significant at $p<0.005$. Adjusted R^2 in each scenario is greater than 91 percent and suggests that the combined variables account for a very high level of variance in post-incident traffic recovery time within each traffic intensity scenario.

Figures 25-27 are scatter plots of simulated recovery times versus the calculated values from regression, for traffic intensity scenarios. The diagrams show a strong correlation between the predicted and simulated recovery times.

Equation 3: Near Capacity Traffic Intensity

$$\text{Log}_e\ T_R = 2.858\text{Rho} + 0.043T_i + 1.285L$$
$$(0.000)^6 \qquad (0.000) \qquad (0.000)$$

$R^2 = 0.999$

Adjusted $R^2 = 0.907$

$N = 14$

Where:
T_R = Recovery time (min)
L = Proportion of lanes closed
N = Number of data points
Rho = *V/C* [0.85-0.95]
T_i = Incident Duration [5, 10,…60]

Equation 4: Moderate Traffic Intensity

$$\text{Log}_e\ T_R = 2.483\textit{Rho} + 0.024T_i + 1.609L$$
$$(0.000) \qquad (0.000) \qquad (0.000)$$

$R^2 = 0.996$

Adjusted $R^2 = 0.977$

$N = 57$

Where:
T_R = Recovery time (min)
L = Proportion of lanes closed
N = Number of data points
Rho = *V/C* [0.60-0.80]
T_i = Incident Duration [5, 10,…60]

Equation 5: Low Traffic Intensity

$$\text{Log}_e\ T_R = 2.855\textit{Rho} + 0.020T_i + 1.506L$$
$$(0.000) \qquad (0.000) \qquad (0.000)$$

$R^2 = 0.999$

Adjusted $R^2 = 0.968$

$N = 36$

Where:
T_R = Recovery time (min)
L = Proportion of lanes closed
N = Number of data points
Rho = *V/C* [0.25-0.50]
T_i = Incident Duration [5, 10,…60]

---

[6] The numbers in parenthesis are probabilities for t-values of coefficients. Probability values less than 0.05 are considered significant at the 5 percent level of significance.

Figure 25: Regression Graph – Near Capacity Traffic Intensity

Recovery Time - High Traffic Intensity
Regression vs. Simulation
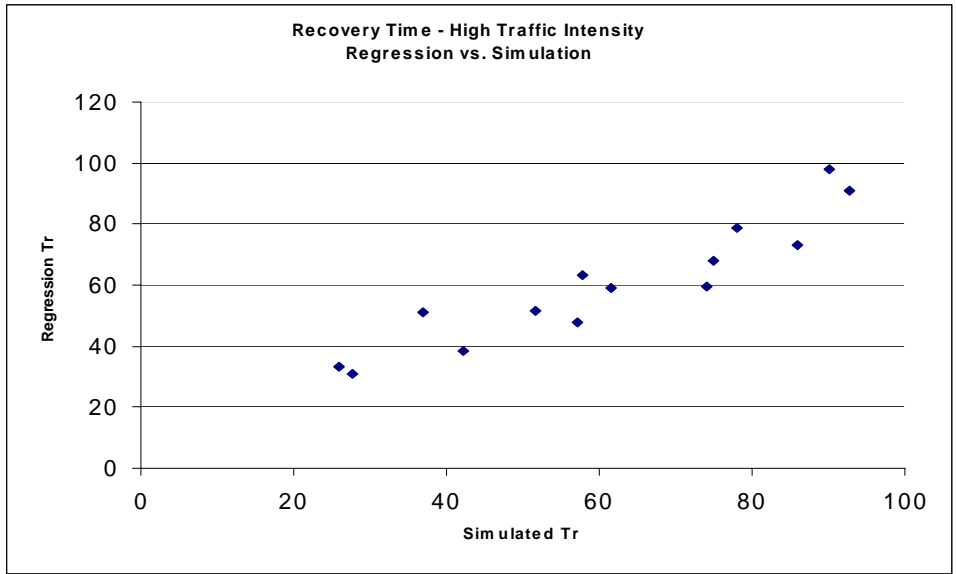
Figure 26: Regression Graph - Moderate Traffic Intensity

Recovery Time - Moderate Traffic Intensity
Regression vs. Simulation
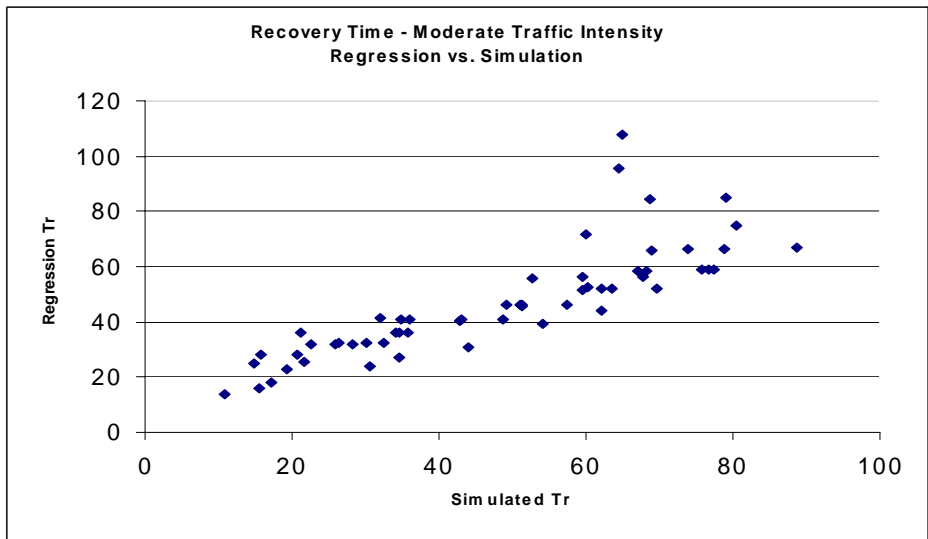
Figure 27: Regression Graph - Low Traffic intensity
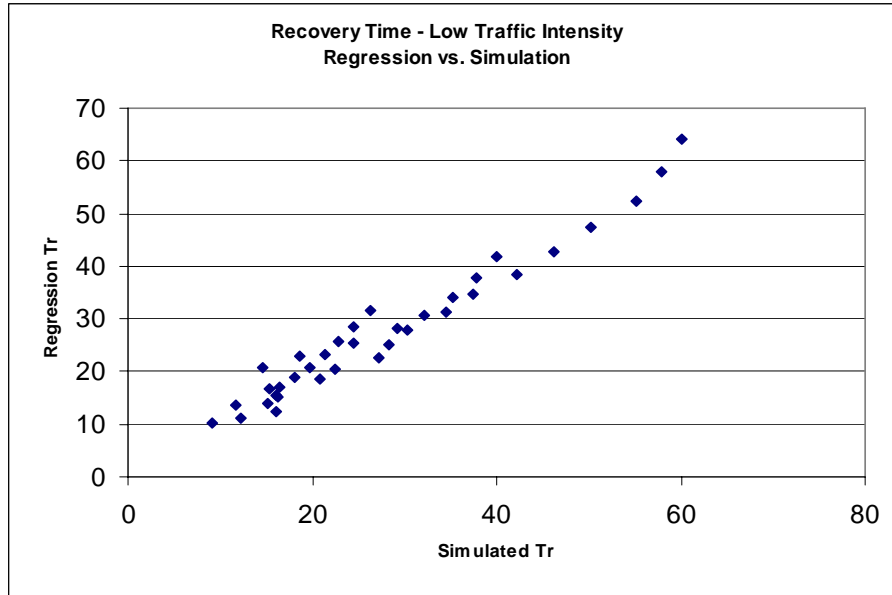
Regression - Lane Scenarios

Equations 7-9 summarize the nonlinear regression analysis of all three lane-blockage scenarios. The R^2 value for all scenarios is extremely high (>0.989) and indicates a strong correlation between the post-incident recovery time and the variables for traffic intensity, incident duration, and proportion of lane blockage. The lowest reported R^2 values are 0.989 for the three-lane-blockage scenario, and 0.997 for the single-lane-blockage scenario. The two-lane-blockage scenario shows an extremely strong correlation between the dependent and independent variables with an R^2 value of 1.00. The results for each scenario is statistically significant at p<0.005. Adjusted R^2 in all lane scenarios is greater than 90 percent and suggests that the combined variables account for a very high level of variance in post-incident traffic recovery time across each lane scenario.

Equation 6: Scenario 1: Three Lanes Blocked

$$\text{Log}_e \, T_R = 4.437 Rho + 0.039 T_i$$

$$\phantom{\text{Log}_e \, T_R =} (0.000) \qquad (0.000)$$

$R^2 = 0.989$

Adjusted $R^2 = 0.976$

$N = 83$

> Where:
> T_R = Traffic recovery time (min)
> *Rho* = V/C (0.25-0.95)
> *Ti* = Incident time (min)
> *N* = Number of data points

Equation 7: Scenario 2: Two Lanes Blocked

$$\text{Log}_e \, T_R = 4.381 Rho + 0.020 T_i$$

$$\phantom{\text{Log}_e \, T_R =} (0.000) \qquad (0.000)$$

$R^2 = 1.00$

Adjusted $R^2 = 0.90$

$N = 12$

Equation 8: Scenario 3: One Lane Blocked

$$\text{Log}_e \, T_R = 3.393 Rho + 0.019 T_i$$

$$\phantom{\text{Log}_e \, T_R =} (0.000) \qquad (0.000)$$

$R^2 = 0.997$

Adjusted $R^2 = 0.897$

$N = 12$

Tables 9-11 summarize the ratio of incident duration to traffic recovery across varying traffic intensity levels or Rho (*v/c*). The ratio is larger for higher levels of Rho (v/c) and lane closure.

At Rho of 0.9, the recovery time is nine times the incident duration when all three lanes are blocked (100 percent closure); six times incident duration for a two-lane blockage (67 percent closure); and three times incident duration when only one lane is blocked (33 percent closure). This means that for a 20-minute incident, recovery time would be 180 minutes for a three-lane blockage; 120 minutes for a two-lane blockage; and 60 minutes for a one-lane blockage. At near capacity levels (Rho 0.95) post-incident recovery time is as high as 15 times the incident duration, meaning that a 5-minute incident will likely result in delays in excess of 75 minutes.

Table 9: Near Capacity Level - Comparison of Regression & Simulated Results

Original Rho ρ^0	Incident Time (min)	Proportion of Lane Blockage	Simulated Recovery Time (min)	Recovery Time From Regression Model (min)	Ratio Of Recovery Time/ Incident Time (Predicted Values)	Ratio Of Recovery Time/ Incident Time (Simulation)
0.95	5	1	75	68	14	**15.0**
0.90	5	1	62	59	12	**12.3**
0.90	10	1	86	73	7	**8.6**
0.90	15	1	93	91	6	**6.2**
0.85	5	1	37	51	10	**7.4**
0.85	10	1	58	63	6	**5.8**
0.85	15	1	78	79	5	**5.2**
0.85	20	1	90	98	5	**4.5**
0.90	10	0.67	57	48	5	**5.7**
0.90	15	0.67	74	59	4	**4.9**
0.85	15	0.67	52	52	3	**3.5**
0.90	10	0.33	28	31	3	**2.8**
0.90	15	0.33	42	38	3	**2.8**
0.85	15	0.33	26	33	2	**1.7**

** Lane blockage is calculated as a proportion of the number of lanes closed to the number of lanes on the corridor.

Table 10: Moderate Traffic Intensity - Comparison of Regression & Simulated Results

Original Rho ρ^0	Incident Time (min)	Proportion of Lane Blockage	Simulated Recovery Time (min)	Recovery Time From Regression Model (min)	Ratio Of Recovery Time/ Incident Time (Predicted Values)	Ratio Of Recovery Time/ Incident Time (Simulation)
0.80	5	1	36	41	8	7.2
0.80	10	1	49	46	5	4.9
0.80	15	1	60	52	3	4.0
0.80	20	1	77	59	3	3.9
0.80	25	1	89	67	3	3.6
0.75	5	1	21	36	7	4.2
0.75	10	1	35	41	4	3.5
0.75	15	1	51	46	3	3.4
0.75	20	1	62	52	3	3.1
0.75	25	1	76	59	2	3.0
0.75	35	1	81	75	2	2.3
0.75	40	1	79	85	2	2.0
0.70	5	1	23	32	6	4.5
0.70	10	1	34	36	4	3.4
0.70	15	1	49	41	3	3.2
0.70	20	1	57	46	2	2.9
0.70	25	1	70	52	2	2.8
0.70	30	1	77	59	2	2.6
0.70	35	1	79	66	2	2.3
0.70	45	1	69	85	2	1.5
0.70	50	1	65	95	2	1.3
0.70	55	1	65	108	2	1.2
0.65	5	1	16	28	6	3.2
0.65	10	1	26	32	3	2.6
0.65	15	1	35	36	2	2.3
0.65	20	1	43	41	2	2.2
0.65	25	1	51	46	2	2.1
0.65	30	1	64	52	2	2.1
0.65	35	1	68	59	2	2.0
0.65	40	1	74	66	2	1.8

Table 11: Moderate Traffic Intensity (cont'd) - Comparison of Regression & Simulated Results

Original Rho ρ^0	Incident Time (min)	Proportion of Lane Blockage	Simulated Recovery Time (min)	Recovery Time From Regression Model (min)	Ratio Of Recovery Time/ Incident Time (Predicted Values)	Ratio Of Recovery Time/ Incident Time (Simulation)
0.60	5	1	15	25	5	3.0
0.60	10	1	21	28	3	2.1
0.60	15	1	28	32	2	1.9
0.60	20	1	36	36	2	1.8
0.60	25	1	43	41	2	1.7
0.60	30	1	51	46	2	1.7
0.60	35	1	60	52	1	1.7
0.60	40	1	67	58	1	1.7
0.60	45	1	69	66	1	1.5
0.80	15	0.67	44	31	2	2.9
0.75	15	0.67	35	27	2	2.3
0.70	15	0.67	31	24	2	2.0
0.80	30	0.67	62	44	1	2.1
0.75	30	0.67	54	39	1	1.8
0.75	45	0.67	68	56	1	1.5
0.70	50	0.67	60	56	1	1.2
0.65	55	0.67	53	56	1	1.0
0.70	60	0.67	60	71	1	1.0
0.80	15	0.33	17	18	1	1.2
0.75	15	0.33	16	16	1	1.0
0.70	15	0.33	11	14	1	0.7
0.80	30	0.33	22	26	1	0.7
0.75	30	0.33	19	23	1	0.6
0.75	45	0.33	33	33	1	0.7
0.70	50	0.33	26	32	1	0.5
0.65	55	0.33	30	32	1	0.5
0.70	60	0.33	32	41	1	0.5

Table 12: Low Traffic Intensity - Comparison of Regression & Simulated Results

Original Rho ρ^0	Incident Time (min)	Proportion of Lane Blockage	Simulated Recovery Time (min)	Recovery Time From Regression Model (min)	Ratio Of Recovery Time/ Incident Time (Predicted Values)	Ratio Of Recovery Time/ Incident Time (Simulation)
0.50	5	1	15	21	4	2.9
0.50	10	1	19	23	2	1.9
0.50	15	1	24	26	2	1.6
0.50	20	1	29	28	1	1.5
0.50	25	1	35	31	1	1.4
0.50	30	1	38	35	1	1.3
0.50	35	1	42	38	1	1.2
0.50	40	1	46	43	1	1.2
0.50	45	1	50	47	1	1.1
0.50	50	1	55	52	1	1.1
0.50	55	1	58	58	1	1.1
0.50	60	1	60	64	1	1.0
0.35	5	1	12	14	3	2.4
0.35	10	1	16	15	2	1.6
0.35	15	1	15	17	1	1.0
0.35	20	1	21	18	1	1.0
0.35	25	1	23	20	1	0.9
0.35	30	1	27	23	1	0.9
0.35	35	1	28	25	1	0.8
0.35	40	1	30	28	1	0.8
0.35	45	1	32	31	1	0.7
0.35	50	1	35	34	1	0.7
0.35	55	1	38	38	1	0.7
0.35	60	1	40	42	1	0.7
0.25	5	1	9	10	2	1.8
0.25	10	1	12	11	1	1.2
0.25	15	1	16	13	1	1.1
0.25	20	1	15	14	1	0.8
0.25	25	1	16	15	1	0.6
0.25	30	1	17	17	1	0.6
0.25	35	1	18	19	1	0.5
0.25	40	1	20	21	1	0.5
0.25	45	1	21	23	1	0.5
0.25	50	1	23	26	1	0.5
0.25	55	1	25	28	1	0.4
0.25	60	1	26	31	1	0.4

CONCLUSION AND DISCUSSION

This study concludes that post-incident recovery time is a nonlinear function of traffic intensity, incident time, and the ratio of lanes closed. Therefore, the SHA can easily estimate the full recovery time after the occurrence of an incident using the formula derived in this report. This research enhances the ability of the SHA to quantify the impact of congestion and delay on the highway network. The regression formula for determining post-incident traffic recovery time will enable state personnel to systematically ascertain the magnitude of traffic congestion conditions along the state highways. In addition, it will be possible to reasonably estimate the effect of proportional lane closures and increasing traffic intensity on congestion buildup.

Simulation results indicate that congestion increases as incident duration increases at all Rho values but increases at faster rates for higher Rho values (Table 4). Within the same incident duration, recovery times increase proportionally, albeit nonlinearly, with traffic intensity. However, as traffic intensity approaches capacity threshold (Rho [ρ^0] = 1), recovery time becomes indefinite (Figures 15-17). Simulation results also indicate that post-incident recovery times return the same or similar values across varying combinations of traffic intensity and incident durations (Table 5).

Analysis of the regression models confirm a nonlinear relationship between recovery time and the independent variables of traffic intensity, incident duration and lane blockage proportion. Disaggregated models based on traffic intensity return the best model for estimating post-incident recovery times with an adjusted R^2 ranging from 91-98 percent.

It is widely thought that recovery time increases by a factor of four for every minute of incident time along a freeway, and this claim has been the basis on which most incident management programs have been implemented. However, this practice does not differentiate between traffic intensity levels along a highway. Tables 9-11 summarize ratios of traffic recovery to incident duration across varying traffic intensity levels. As expected, the ratio is very high for higher levels of traffic intensity and lane closure.

The results described herein are based on a simple highway corridor without on-ramps, off-ramps, or other bottlenecks (such as lane drops and grades). The traffic was assumed to be static during the simulation period. In addition, only one isolated incident per time and space was considered, i.e., the impact of multiple incidents on congestion and recovery time was not included. Therefore, the estimated traffic-recovery times are considered to be conservative and may be shorter than the actual recovery times. Incidents could also engender rubbernecking behavior, which further deteriorates the prevailing congested conditions.

The above limitations could all reduce the ability to generalize the results across urban freeway networks. Further work would be required to broaden the applicability of the model. Notwithstanding, the model is expected to serve as a valuable guide for incident managers and decision makers assessing the ramifications of delayed response to highway incidents and developing improved incident management methods. Secondary

analysis of the simulation results can also be done to determine some environmental and economic costs associated with specified scenarios of freeway incidents investigated in this study.

Appendices

Appendix 1: Summary of Morning Peak Hour Volumes on the JFX Corridor[7]

Facility Name	NBT	NBR	NBL	SBT	SBR	SBL	EBT	EBR	EBL	WBT	WBR	WBL
JFX/President Street	1502	235	200	2673	1429	1610						
Fayette Street							215	155		314	590	91
Fallsway-JFX	120										107	
Orleans Street							1679	150	195	1967	113	160
Madison Street										1770	102	75
Monument Avenue							1455	135	145			
On JFX Ramp 2	544											
Exit 3 Off ramp JFX	159											
On JFX Ramp 3	156											
Greenmount Avenue	365	12	80	1727	64	65						
Chase Street							137	22	36	256	92	24
Fallsway	121	128		84		55						
Gay Street							640	128	128	-	-	-
On JFX Ramp 2	549											
Fallsway	161	30										
Centre Street							1940	853	357			
Fallsway	243	95	123									
Madison Street										709	61	
On JFX Ramp 3											425	
Exit 3 Mainstream	2680											
Fallsway	243	74	118									
Chase Street							73	-	17	109	45	
Biddle Street							359	42	18			
Fallsway	200	18										
Guilford Avenue				432		153						
Preston Street										533	110	133
Guilford & Fallsway	173	-	39	397	40							
North Avenue							1034	816	79	-	-	81
Maryland				790	148	148						
On JFX Ramp 3	156											
On JFX at Exit 4/5	1003											
Exit 5 Mt. Royal Avenue				1282								
Exit 4 SBR to Mt. Royal					230							
Exit 4 SBL to St. Paul						725						
Exit 4 Main Stream				7120								
On JFX Ramp Exit 3				185								
Eager Street							125					
Center Street							784	69				
Exit 3 Guilford Avenue				455		964						
Madison Street										822		261
Guilford Avenue				1684	198							
Centre Street							716	420				
St. Paul Street				1871		725						
Centre Street							812	156				
Cathedral Street				808		84						
JFX Exit 2 Mt. Pleasant					174							
SBL on Holiday Street						123						
Exit 5 Main Stream JFX	3683			8195								
Exit 2 Main Stream				5886								
Centre Street							1940	235				
Guilford Avenue				455		964						
Exit 3 Main Stream				5701								
Exit 1 Main Stream				5712								

7 Traffic Count Data Collected by Morgan State University, May - September 2007

Appendix 2: Calculation of Effective Rho Values [Three Lanes Blocked]

			Incident Time (min)	5	10	15	20	25	30	35	40	45	50	55	60
			Incident Time (sec)	300	600	900	1200	1500	1800	2100	2400	2700	3000	3300	3600
Potential Capacity (Maximum) for 2.5 hours – 18,000 vehicles			**End Red Time (sec)**	2100	2400	2700	3000	3300	3600	3900	4200	4500	4800	5100	5400
Initial_Rho (V/C) [ρ^0]	3-Lane (1-hr) Volume @ Initial Rho	Demand @ start of Sim	Effective Rho Capacity [ρ^1]	17,400	16,800	16,200	15,600	15,000	14,400	13,800	13,200	12,600	12,000	11,400	10,800
0.95	6840	17,100	Effective Rho value [ρ^2]	1.0	1.0	1.0	1.1	1.1	1.2	1.2	1.3	1.3	1.4	1.5	1.5
0.9	6480	16,200		0.9	1.0	1.0	1.0	1.1	1.1	1.1	1.2	1.2	1.3	1.3	1.4
0.85	6120	15,300		0.9	0.9	0.9	1.0	1.0	1.0	1.1	1.1	1.1	1.2	1.2	1.3
0.8	5760	14,400		0.8	0.8	0.9	0.9	0.9	1.0	1.0	1.0	1.1	1.1	1.1	1.2
0.75	5400	13,500		0.8	0.8	0.8	0.8	0.9	0.9	0.9	0.9	1.0	1.0	1.0	1.1
0.7	5040	12,600		0.7	0.7	0.8	0.8	0.8	0.8	0.8	0.9	0.9	0.9	0.9	1.0
0.65	4680	11,700		0.7	0.7	0.7	0.7	0.7	0.7	0.8	0.8	0.8	0.8	0.9	0.9
0.6	4320	10,800		0.6	0.6	0.6	0.7	0.7	0.7	0.7	0.7	0.7	0.8	0.8	0.8
0.5	3600	9,000		0.5	0.5	0.5	0.5	0.5	0.6	0.6	0.6	0.6	0.6	0.6	0.6
0.35	2520	6,300		0.4	0.4	0.4	0.4	0.4	0.4	0.4	0.4	0.4	0.4	0.4	0.4
0.25	1800	4,500		0.3	0.3	0.3	0.3	0.3	0.3	0.3	0.3	0.3	0.3	0.3	0.3

Note: See Equation1 for calculation of effective Rho [ρ^1].

Appendix 3: Sample Spreadsheet of Post-Incident Recovery Times [Three Lanes Blocked]

<u>SCENARIO 1 - 3-LANES -ALL RANDOM NUMBER SEEDS</u>

2100	2400	2700	3000	3300	3600

INCIDENT TIME

RHO	SEED	5MIN
0.95	sim 1	111
	sim 2	68
	sim 3	64
	sim 4	55
	sim 5	48
	sim 6	105
AVG Recovery Time	**AVG**	**75**

*** Recovery time not clearly evident

INCIDENT TIME

Initial RHO	SEED	5MIN	10MIN	15MIN
0.9	sim 1	30	61	93
	sim 2	65	99	72
	sim 3	51	75	102
	sim 4	97	85	***
	sim 5	45	97	105
	sim 6	82	100	***
AVG Recovery Time	**AVG**	**62**	**86**	**93**

INCIDENT TIME

Initial RHO	SEED	5MIN	10MIN	15MIN	20MIN	25MIN
0.85	sim 1	24	62	62	87	88
	sim 2	47	***	96	***	***
	sim 3	27	46	73	***	88
	sim 4	61	72	96	***	***
	sim 5	35	50	71	88	89
	sim 6	30	60	70	96	86
AVG Recovery Time	**AVG**	**37**	**58**	**78**	**90**	**87**

Appendix 4: Regression Results - All Lane Scenarios [Constant = Zero]

| SUMMARY OUTPUT | | Regression-all-Constant = Zero | | | | | | | |

Regression Statistics	
Multiple R	0.929
R Square	**0.863**
Adjusted R Square	**0.851**
Standard Error	0.215
Observations	107

ANOVA

	df	SS	MS	F	Significance F
Regression	3	30.401	10.134	218.762	0.000
Residual	104	4.818	0.046		
Total	107	35.219			

	Coefficients	Standard Error	t Stat	P-value	Lower 95percent	Upper 95percent	Lower 95percent	Upper 95percent
Intercept	0.000	#N/A	#N/A	#N/A	#N/A	#N/A	#N/A	#N/A
ORIG RHO ?0	2.819	0.072	39.261	0.000	2.677	2.962	2.677	2.962
INCIDENT TIME	0.021	0.001	18.661	0.000	0.019	0.024	0.019	0.024
LANE BLOCKAGE	1.475	0.057	25.812	0.000	1.361	1.588	1.361	1.588

Appendix 5: Regression Results – Near Capacity Traffic Intensity

SUMMARY OUTPUT					Regression - Traffic Intensity Near Capacity ($0.8 < Rho < 1.0$)			

Regression Statistics	
Multiple R	0.999
R Square	**0.999**
Adjusted R Square	**0.907**
Standard Error	0.171
Observations	14

ANOVA

	df	SS	MS	F	Significance F
Regression	3	230.474	76.825	2630.199	0.000
Residual	11	0.321	0.029		
Total	14	230.795			

	Coefficients	Standard Error	t Stat	P-value	Lower 95percent	Upper 95percent	Lower 95percent	Upper 95percent
Intercept	0.000	#N/A	#N/A	#N/A	#N/A	#N/A	#N/A	#N/A
ORIG RHO ?0	2.858	0.228	12.551	0.000	2.357	3.360	2.357	3.360
INCIDENT TIME	0.043	0.010	4.334	0.001	0.021	0.065	0.021	0.065
LANE BLOCKAGE	1.285	0.171	7.528	0.000	0.910	1.661	0.910	1.661

Appendix 6: Regression Results – Moderate Traffic Intensity

SUMMARY OUTPUT					Regression - Traffic Intensity Moderate (0.5<*Rho*≤0.80)				

Regression Statistics	
Multiple R	0.998
R Square	**0.996**
Adjusted R Square	**0.977**
Standard Error	0.242
Observations	57

ANOVA

	df	SS	MS	F	Significance F
Regression	3	815.338	271.779	4655.445	0.000
Residual	54	3.152	0.058		
Total	57	818.491			

	Coefficients	Standard Error	t Stat	P-value	Lower 95percent	Upper 95percent	Lower 95percent	Upper 95percent
Intercept	0.000	#N/A	#N/A	#N/A	#N/A	#N/A	#N/A	#N/A
ORIG RHO ?0	2.483	0.170	14.577	0.000	2.141	2.824	2.141	2.824
INCIDENT TIME	0.024	0.002	12.111	0.000	0.020	0.028	0.020	0.028
LANE BLOCKAGE	1.609	0.114	14.105	0.000	1.380	1.837	1.380	1.837

Appendix 7: Regression Results – Low Traffic Intensity

SUMMARY OUTPUT		Regression - Traffic Intensity Low (0.25≤*Rho*≤0.5)							

Regression Statistics	
Multiple R	0.999
R Square	**0.999**
Adjusted R Square	**0.968**
Standard Error	0.124
Observations	36

ANOVA

	df	SS	MS	F	Significance F
Regression	3	380.541	126.847	8264.768	0.000
Residual	33	0.506	0.015		
Total	36	381.048			

	Coefficients	Standard Error	t Stat	P-value	Lower 95percent	Upper 95percent	Lower 95percent	Upper 95percent
Intercept	0.000	#N/A	#N/A	#N/A	#N/A	#N/A	#N/A	#N/A
ORIG RHO ?0	2.855	0.201	14.204	0.000	2.446	3.264	2.446	3.264
INCIDENT TIME	0.020	0.001	17.130	0.000	0.018	0.023	0.018	0.023
LANE BLOCKAGE	1.506	0.086	17.544	0.000	1.331	1.681	1.331	1.681

Appendix 8: Regression Results – Three-Lanes Blocked Scenario [Constant = Zero]

SUMMARY OUTPUT		Three-Lane Scenario Constant = Zero							

Regression Statistics	
Multiple R	0.994
R Square	**0.989**
Adjusted R Square	**0.976**
Standard Error	0.393
Observations	83

ANOVA

	df	SS	MS	F	Significance F
Regression	2	1107.242	553.621	3592.585	0.000
Residual	81	12.482	0.154		
Total	83	1119.724			

	Coefficients	Standard Error	t Stat	P-value	Lower 95percent	Upper 95percent	Lower 95percent	Upper 95percent
Intercept	0.000	#N/A	#N/A	#N/A	#N/A	#N/A	#N/A	#N/A
ORIG RHO ?0	4.437	0.105	42.074	0.000	4.227	4.646	4.227	4.646
INCIDENT TIME	0.039	0.002	19.026	0.000	0.035	0.043	0.035	0.043

Appendix 9: Regression Results – Two-Lanes Blocked Scenario [Constant = Zero]

SUMMARY OUTPUT		Two-Lane Scenario Constant = Zero						

Regression Statistics	
Multiple R	1.000
R Square	**1.000**
Adjusted R Square	**0.900**
Standard Error	0.081
Observations	12

ANOVA

	df	SS	MS	F	Significance F
Regression	2	188.925	94.463	14365.179	0.000
Residual	10	0.066	0.007		
Total	12	188.991			

	Coefficients	Standard Error	t Stat	P-value	Lower 95percent	Upper 95percent	Lower 95percent	Upper 95percent
Intercept	0.000	#N/A	#N/A	#N/A	#N/A	#N/A	#N/A	#N/A
ORIG RHO ?0	4.381	0.053	82.999	0.000	4.264	4.499	4.264	4.499
INCIDENT TIME	0.020	0.001	16.538	0.000	0.017	0.022	0.017	0.022

Appendix 10: Regression Results – One-Lane Blocked Scenario [Constant = Zero]

SUMMARY OUTPUT	One-Lane Scenario Constant = Zero							

Regression Statistics	
Multiple R	0.998
R Square	**0.997**
Adjusted R Square	**0.897**
Standard Error	0.197
Observations	12

ANOVA

	df	SS	MS	F	Significance F
Regression	2	121.232	60.616	1568.553	0.000
Residual	10	0.386	0.039		
Total	12	121.618			

	Coefficients	Standard Error	t Stat	P-value	Lower 95percent	Upper 95percent	Lower 95percent	Upper 95percent
Intercept	0.000	#N/A	#N/A	#N/A	#N/A	#N/A	#N/A	#N/A
ORIG RHO ?0	3.393	0.128	26.517	0.000	3.108	3.678	3.108	3.678
INCIDENT TIME	0.019	0.003	6.496	0.000	0.012	0.025	0.012	0.025

REFERENCE

AbTech Corporation. *ModelQuest 4.0 User Manual*, Charlottesville, VA, 1999

Ahmed, S. A., & Cook, A. R. (1980). Application of Time Series Analysis Techniques to Freeway Incident Detection, *Transportation Research Record,* 682, TRB, Washington, D.C., pp. 19-21.

Al-Deek, H. (1999). "Implementation of Incident Detection Algorithms" Summary of Final Report, WPI 0510672, Florida Department of Transportation.

Bertini, R. L., & Myton, A. M. (2005). "Using PeMS Data to Empirically Diagnose Freeway Bottleneck Locations in Orange County", California, *84th Annual Meeting of the Transportation Research Board*.

Bertini, R.L., Rose, M.W., & Geneidy, A. E. (2005). "Using Archived ITS Data Sources to Measure the Effectiveness of a Freeway Incident Response Program", *84th Annual Meeting of the Transportation Research Board*.

Bertini, R. Tantiyanugulchai, S. Anderson, E. Lindgren, & R. Leal, M. (2001). Evaluation of Region 2 Incident Response Program Using Archived Data. Portland State University, *Transportation Research Group*, Research Report.

Carvell, James D., Kevin Blake, Jerry Ullman, Katherine Fitzpatrick, Lewis Nowlin, & Christopher Brehmer. (1997). Freeway Management Handbook, U.S. Department of Transportation, Federal Highway Administration.

Chang, Gang L., & Rochon, Steven. (2006). Performance Evaluation of CHART – The Real Time Incident Management System in Year 2005, Final Report.

Chang, E.C., & Huang, K. (1993). Freeway Incident Management Expert System Design, *Transportation Research Board*, Washington, D.C.

Chen, C., K. Petty, A. Skabardonis, P. Varaiya, & Z. Jia (2001). "Freeway Performance Measurement System: Mining Loop Detector Data," Paper 01-2354, Presented at the 80th TRB Annual Meeting, Washington DC.

Dunn, W., & Latoski, S. (2003). Safe and Quick Clearance of Traffic Incidents, NCHRP Synthesis 318, *Transportation Research Board*.

Giuliano, G. (1989). Incident Characteristics, Frequency, and Duration on a High Volume Urban Freeway, *Transportation Research*, V. 23A, pp. 387-36.

Gupta, A., Maslanka, V., & Spring, G.S. (1992). Development of a prototype KBES in the management of congestion on the Massachusetts Turnpike, *Presentation at annual meeting of the Transportation Research Board*.

Hobeika, A.G. (1996). Real-time Diversion Strategies for Automated Wide-Area Incident Management, Virginia Polytechnic Institute, Center for Transportation Research.

Hobeika, A.G. & Sudheer Dhulipala (2004). Estimation of Travel Times on Urban Freeways under Incident Conditions, *Transportation Research Record*: Journal of the Transportation Research Board 1867, TRB, National Research Council, Washington D.C., pp. 97-106.

Jain, S., & McLean, C. (2006). An Integrated Framework for Modeling and Simulation for Incident Management, *Journal of Homeland Security and Emergency Management*, Volume 3, Issue 1.

Law, Averill M. & Ketton, David W. (2000). Simulation Modeling and Analysis. Mc Graw Hill Boston.

Madanat, S. (1996). The Sequential Hypothesis Testing Based Freeway Incident Response, presented at 1996 meeting of the Transportation Research Board, Washington, D.C.

May, A.D., et al. (1991). "Integrated System of Freeway Corridor Simulation Models," *Transportation Research Record* No. 1320.

Ringert, J. and Thomas Urbanik II. Study of Freeway Bottlenecks in Texas. (1193). In *Transportation Research Record*: Journal of the Transportation Research Board 1398, TRB, National Research Council, Washington D.C., pp. 31-41.

Nathanail, T. and Zografos, K. G. (1995). A framework for Integrating Real Time Information and Decision Support System for Incident Management Operations, International Symposium on Automotive Technology and Automation, pp. 555-563.

Nee, J. and Hallenbeck, M. (2001). Evaluation of the Service Patrol Program in the Puget Sound Region. Report WARD 518.1. FHWA, U.S. Department of Transportation.

Nathanail, T., and Zografos, K. (1995). A Framework for Integrating Real Time Information and Decision Support System for Incident Management Operations, International Symposium on Automotive Technology and Automation (Stuttgart), pp. 555-563.

Nathanail, T. and Zografos, K. (1994). Simulation of freeway incident restoration operations, pp. 229-232, Fifth Vehicle Navigation and Information Systems Conference (Yokohama, Japan).

Olmstead, T. (2001). Freeway Management Systems and Motor Vehicle Crashes: A Case Study of Phoenix, Arizona, Accident Analysis and Prevention 33, pp. 433–447.

Quiroga, C., Hamad, K., and Park, E. (2005). Incident Evaluation Procedures and Implementation Requirements, Research Report 0-4745-2. Draft, Texas Department of Transportation, Austin, Texas.

Roper, D. H. (1990). "Freeway Incident Management", NCHRP 156, Washington, D.C.: Transportation Research Board.

Skabardonis, A. Petty, K. Varaiya, P. and Bertini, R. (1998). Evaluation of the Freeway Service Patrol (FSP) in Los Angeles. PATH Research Report UCB-ITS-PRR-98-31 University of California, Berkley.

Skabardonis, A., et al, (1996). "The I-880 Field Experiment: Database Development and Incident Delay Estimation Procedures," *Transportation Research Record* No, 1554.

Smith, Kevin W. and Brian L. Smith. Forecasting the Clearance Time of Freeway Accidents. Research Report No. UVACTS-15-0-35, Center for Transportation Studies at the University of Virginia.2001.

Sullivan, E.C. (1997). New Model for Predicting Freeway Incidents and Incidents Delays, *Journal of Transportation Engineering*, V.123, pp 267-275.

Sung-Wai, Sabina Y., Chue. R. Long and Lee Der-Horng. A Laboratory Platform for Incident Management Simulation. *Journal of the Institution of Engineers,* Singapore, Vol. 44, Iss.2, 2004, pp. 55-70.

Suttayamully, S. Hadipriono, F., and Nemeth, Z.A. (1995). Knowledge Acquisition, Representation, and Knowledge Base Development of Intelligent Traffic Evaluator for Prompt Incident Diagnosis, pp. 101- 111, *Transportation Research Record* 1497.

Zhang, H. and Ritchie, S.G. (1992). A Real-Time Decision-Support System for Freeway Management and Control, pp. 39-58, International Conference on Artificial Intelligence Applications in Transportation, Ventura, California.

Zografos, K.G., T. Nathanail, and Michalopoulos, P.G. (1993). Analytical framework for minimizing freeway-incident response time, V. 119, pp. 535-549, *Journal of Transportation Engineering*.